

Journal Pre-proofs

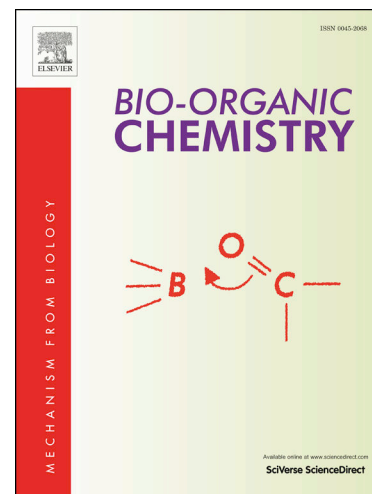
Novel molecular discovery of promising amidine-based thiazole analogues as potent dual Matrix Metalloproteinase-2 and 9 inhibitors: Anticancer activity data with prominent cell cycle Arrest and DNA fragmentation analysis effects

Abdelsattar M. Omar, Jürgen Bajorath, Saleh Ihmaid, Hany M. Mohamed, Ahmed M. El-Agrody, Ahmed Mora, Moustafa E. El-Araby, Hany E.A. Ahmed

PII: S0045-2068(20)31289-X
DOI: <https://doi.org/10.1016/j.bioorg.2020.103992>
Reference: YBIOO 103992

To appear in: *Bioorganic Chemistry*

Received Date: 28 April 2020
Revised Date: 20 May 2020
Accepted Date: 30 May 2020



Please cite this article as: A.M. Omar, J. Bajorath, S. Ihmaid, H.M. Mohamed, A.M. El-Agrody, A. Mora, M.E. El-Araby, H.E.A. Ahmed, Novel molecular discovery of promising amidine-based thiazole analogues as potent dual Matrix Metalloproteinase-2 and 9 inhibitors: Anticancer activity data with prominent cell cycle Arrest and DNA fragmentation analysis effects, *Bioorganic Chemistry* (2020), doi: <https://doi.org/10.1016/j.bioorg.2020.103992>

This is a PDF file of an article that has undergone enhancements after acceptance, such as the addition of a cover page and metadata, and formatting for readability, but it is not yet the definitive version of record. This version will undergo additional copyediting, typesetting and review before it is published in its final form, but we are providing this version to give early visibility of the article. Please note that, during the production process, errors may be discovered which could affect the content, and all legal disclaimers that apply to the journal pertain.

Novel molecular discovery of promising amidine-based thiazole analogues as potent dual Matrix Metalloproteinase-2 and 9 inhibitors: Anticancer activity data with prominent cell cycle Arrest and DNA fragmentation analysis effects

Abdelsattar M. Omar,^{a,b,*} Jürgen Bajorath,^c Saleh Ihmaid,^{*d} Hany M. Mohamed,^{e,f} Ahmed M. El-Agrody,^f Ahmed Mora,^f Moustafa E. El-Araby,^a Hany E. A. Ahmed^{d,g}

^a Pharmaceutical Chemistry Department, Faculty of Pharmacy, King Abdulaziz University, Jeddah 21589, Saudi Arabia

^b Ph Journal Pre-proofs t

^c Department of Life Science Informatics, Bonn-Aachen International Center for Information Technology, Rheinische Friedrich-Wilhelms-Universität Bonn
Endenicher Allee 19c, D-53115 Bonn, Germany

^d Pharmacognosy and Pharmaceutical Chemistry Department, College of Pharmacy, Taibah University, Al-Madinah Al-Munawarah, Saudi Arabia

^e Chemistry Department, Faculty of Science, Jazan University, Jazan 45142, Saudi Arabia

^f Chemistry Department, Faculty of Science, Al-Azhar University, Nasr City, Cairo, 11884, Egypt

^g Pharmaceutical Organic Chemistry Department, Faculty of Pharmacy, Al-Azhar University, 11884 Nasr City, Cairo, Egypt

*Corresponding author.

E-mail address: AMO; asmansour@kau.edu.sa, SKI; saleh_ihmaid@yahoo.com.au

[‡] These authors contributed equally to this work

Abstract

Thiazole derivatives are known to possess various biological activities such as antiparasitic, antifungal, antimicrobial and antiproliferative activities. Matrix metalloproteinases (MMPs) are important protease target involved in tumor progression including angiogenesis, tissue invasion, and migration. Therefore, MMPs have also been reported as potential diagnostic and prognostic biomarkers in many types of cancer. Herein, new aryl thiazoles were synthesized and evaluated for their anticancer effects on a panel of cancer cell lines including the invasive MDA-MB-231 line. Some of these compounds showed IC₅₀ values in the submicromolar range in anti-proliferative assays. In order to examine the relationship between their anticancer activity and MMPs targets, the compounds were evaluated for their inhibitory effects on MMP2 and 9. That data obtained revealed that most of these compounds were potent dual MMP-2/9 inhibitors at nanomolar concentrations. Among these, 2-(1-(2-(2-((*E*)-4-iodobenzylidene)hydrazineyl)-4-methylthiazol-5-yl)ethylidene)hydrazine-1-carboximidamide (**4a**) was the most potent non-selective dual MMP-2/9 inhibitor with inhibitory concentrations of 56 and 38 nM respectively. When compound **4a** was tested in an MDA-MB-231, HCT-116, MCF-7 model, it effectively inhibited tumor growth, strongly induced cancer cell apoptosis, inhibit cell migration, and suppressed cell cycle progression leading to DNA fragmentation. Taken together, the results of our studies indicate that the newly discovered thiazole-based MMP-2/9 inhibitors have significant potential for anticancer treatment.

Keywords: Structure-based design; 2-aminothiazole; amidine; MMP-2/9 inhibition; anticancer activity.

1. Introduction

Cancer is a major medical concern and among the most frequent causes for death worldwide [1, 2] Although the survival rates for certain cancers have increased over the past decades due to early diagnosis and development of innovative treatments, effective therapeutic strategies for the successful treatment of advanced cancers are still lacking [3]. There is clinical evidence that about 80% of cancer-related deaths are due to a lack of early diagnosis [4,5]. For advanced cancers, conventional methods of treatment such as radiotherapy and chemotherapy are no longer efficacious because they destroy normal cells and malignant cells at comparable rates, leading to severe toxicity with only small to moderate therapeutic improvements [6, 7]. On the other hand, progress has been made with targeted therapies such as broad-spectrum kinase inhibition for the treatment of advanced cancers [8]. For targeted anticancer therapies, thiazoles are among the most versatile compound classes. The thiazole heterocycle is found in many anticancer agents and different studies have shown that thiazole based compounds induce a variety of therapeutically relevant pharmacological effects [9-16]. The thiazole nucleus originates from the reaction of the thiosemicarbazone moiety and thiazole-based agents display broad-spectrum antiproliferative effects and

low toxicity in preclinical studies [17,18]. The thiosemicarbazone precursor of the thiazole heterocycle also exhibits anticancer effects. The antitumor activity of thiosemicarbazones appears to be generally due to inhibition of DNA synthesis due to modification of the reductive conversion of ribonucleotides to deoxyribonucleotides [19,20].

Matrix metalloproteinases (MMPs) are a family of extracellular zinc- and calcium-dependent neutral endopeptidases including a number of closely related isoforms playing a crucial role in degradation of extracellular matrix components, tissue remodeling and the pathogenesis of major diseases [21]. MMPs are involved in Journal Pre-proofs sis, cellular variation, and wound healing [22]. Furthermore, they are also implicated in inflammation, tumor cells proliferation, and other diseases [23]. MMPs play a critically important role in the remodeling and repair of physiological tissues, but their overexpression lead to a variety of pathologies including aberrant cell proliferation and cancer [24]. Therefore, inhibiting MMPs is an attractive approach for treating a variety of diseases. For example, many inhibitors of MMP-2 have been proven to prevent tumor growth, some of which have reached clinical trials [25]. Representative examples include compounds 1-4 (**Fig. 1**) that were tested as anticancer agents [26,27]. In drug discovery, a number of MMP isoforms including MMP-2, MMP-3, MMP-8, MMP-9, MMP-12 and MMP-14 are considered as anti-targets whereas MMP-2 and MMP-9 (in the following abbreviated MMP-2/9), the focal points of our study, are regarded as anticancer targets for blocking the proliferation of tumor cells [28,29].

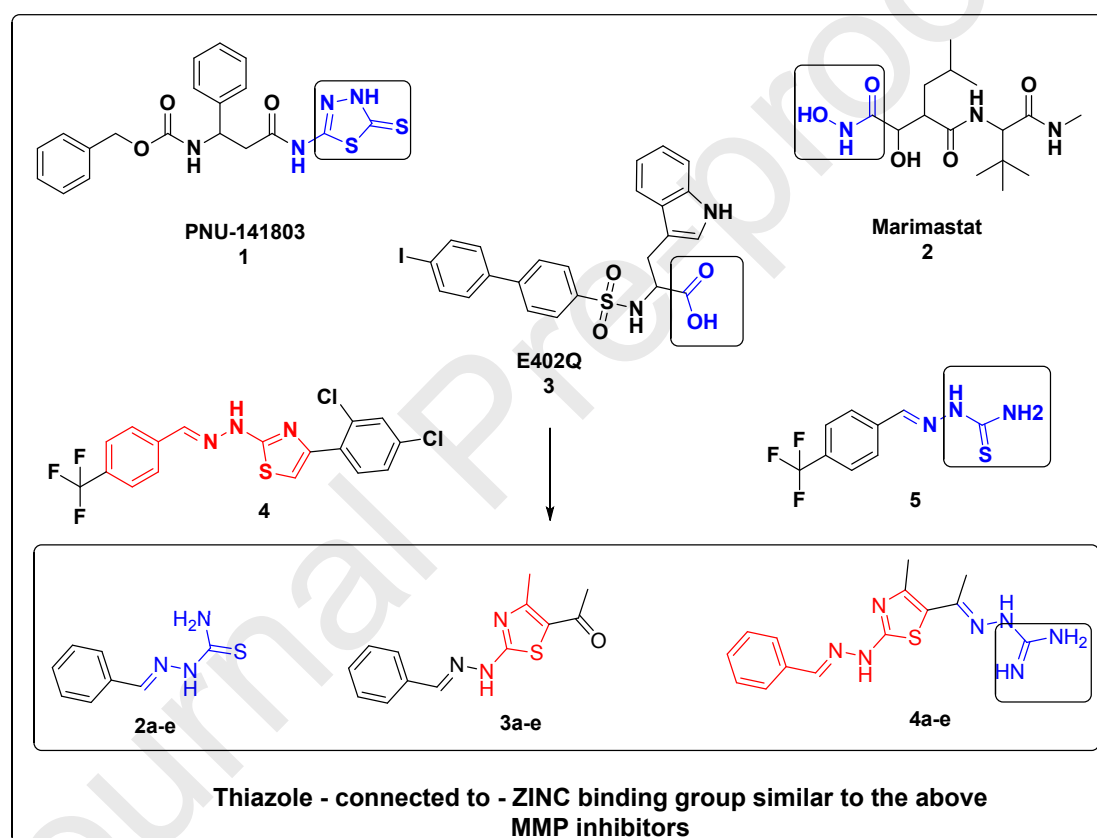


Fig. 1. General strategy for the design of thiazole-based hybrid compounds as MMP-2/9 inhibitors focusing on zinc binding groups (ZBGs) in reference drugs.

Previously, a series of pyrazothiazoles linked to salicylaldehyde were reported as anticancer agents targeting MMP-2/9 [30]. Considering these previous studies, the general anticancer activity of thiazole and thiosemicarbazide moieties, structure-based analyses of the reference compounds in (**Fig. 1**) was carried out as presented below. Our analysis has led to molecular hybridization of the thiazole heterocycle and the hydrophilic metal conjugating guanidine moiety as a zinc binding group in the design of new MMP-2/9 inhibitors targeting their catalytic zinc site in analogy to carbamate- or carboxylate containing clinical inhibitors. Our thiazole/guanidine hybrid design was further extended with different aromatic fragments via a polar linker NH-N=C that contribute to MMP binding of analogues by targeting pockets in the active site region [27]. These newly designed and synthesized compounds with their terminal hydrophilic zinc-chelating substructure were found to be potent MMP-2/9 inhibitors and were also tested for their ability to decrease proliferation of different invasive and non-invasive cancers compared to normal tissues. Antiproliferative activity of our best inhibitors was confirmed for three human cancer cell lines including invasive breast cancer cell line (MDA-MB-231), human colon cancer (HCT-116), and mammary gland breast cancer (MCF-7) compared to two normal cell lines, namely, human keratinocytes cell line (HaCaT) and human diploid fibroblasts (WI-38). In light of recently growing evidence show that MMPs have both proteolytic and non-proteolytic intracellular functions [31], we also examined

the possible relationship between the combination of internal thiazole with amidine terminus on MMP inhibitory activity of the new compounds and cell apoptosis or cell cycle arrest. Furthermore, SAR features of our inhibitors accentuated the influence of substituents at different positions on the antitumor activity.

2. Results and discussion

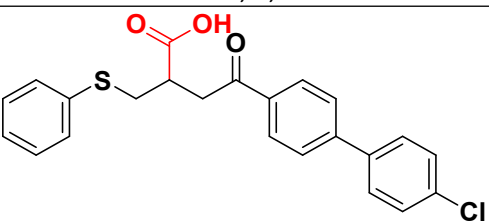
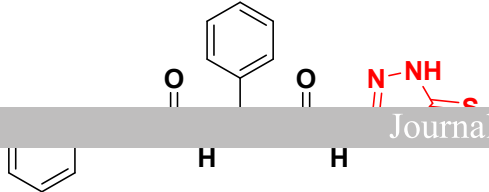
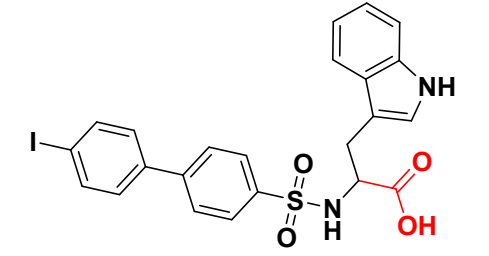
2.1. Structure-based scaffold and compound design

MMP inhibitors (MMPIs) typically act by chelating the catalytic zinc (Zn^{2+}) cation, which is a hallmark of MMPIs used as anticancer agents.[32] Some reports indicated that MMPIs act by inhibiting cancer cell growth whereas others reported that MMPIs function by decreasing tumor proliferation through induction of apoptosis via release of $TNF\alpha$ or TRAIL (tumor necrosis factor related apoptosis inducing ligand) from their membrane bound inactive form [32]. MMPs are highly expressed in human cancer and implicated in every stage of cancer development.[32] The cancer cell secretes various agents such as interferon, interleukins and growth factors as well as extracellular MMP inductor which stimulate the surrounding host cell to generate MMPs required for the tumor cell [32].

The structure-based design of our 2-aminothiazole derivative MMP-2/9 dual inhibitors commenced by analyzing a set of different selective MMP inhibitors [33,34] and their binding characteristics in the active sites of MMP-2 (using X-ray structure entry PDB 2SUN) and MMP-9 (PDB 2OW0), respectively. As shown in (Table 1), different zinc binding groups (ZBGs) of reference inhibitors were analyzed including hydroxamic acid, thiols, carboxylates and phosphonic acid [21,35]. Among these groups, preference was assigned to the Zn^{2+} binding features of hydroxamic acid. In the MMP active site, the NH and deprotonated OH groups of hydroxamic acid form well-defined hydrogen bonds with Ala and Glu residues [35,36].

Table 1. Structural analyses of ZBGs from natural and synthetic MMP-2/9 inhibitors.

Ligand	ZBG
<p>Non-selective MMP inhibitor</p>	<i>N</i> -hydroxyacetamide
<p>Non-selective MMP inhibitor</p>	<i>N</i> -hydroxyacetamide
<p>Selective MMPs 2, 3, 9, 13, and 14 inhibitor</p>	<i>N</i> -hydroxythiomorpholine-3-carboxamide
<p>Selective MMPs 2, 3, and 9 inhibitor</p>	<i>N</i> -hydroxyacetamide
<p>Selective MMPs 2, 3, and 9 inhibitor</p>	2-mercaptopropanamide

<p>Selective MMPs 2, 3, and 9 inhibitor</p>  <p>Selective MMPs 2, 3, and 9 inhibitor</p>	Acetic acid
 <p>Selective MMP3 inhibitor</p>	Acetic acid
 <p>Selective MMP9 inhibitor</p>	Acetic acid

The table lists a variety of MMP reference inhibitors containing different ZGBs (colored in red).

X-ray structures of MP-2/9 are shown in (**Fig. 2**). (**Fig. 2A**) reveal that the thiazolidine-based inhibitor bound to MMP-2 formed a monodentate interaction with the zinc cation in the catalytic site through the sulfhydryl group that was further stabilized by intermolecular H₂O-mediated hydrogen bonds. In the active site of MMP-2, additional hydrogen bonds were formed through the two imide linkers with involving residue Glu 202, His 205, Ala 167, Tyr 168 and Ala 169. Furthermore, hydrophobic subsites were expected to accommodate terminal lipophilic or aromatic groups of inhibitors. (**Fig. 2B**) shows that hydroxamate-based inhibitor bound to MMP-9 formed a bidentate interaction with the catalytic zinc site and well-defined hydrogen bonds with the active site of MMP-9 involving residues Gly 186, Pro 421, Glu 402, Ala 189, Leu 188 and Tyr 423. This map of interactions are derived from the analyses of both crystal structures was consistent with previous findings [37].

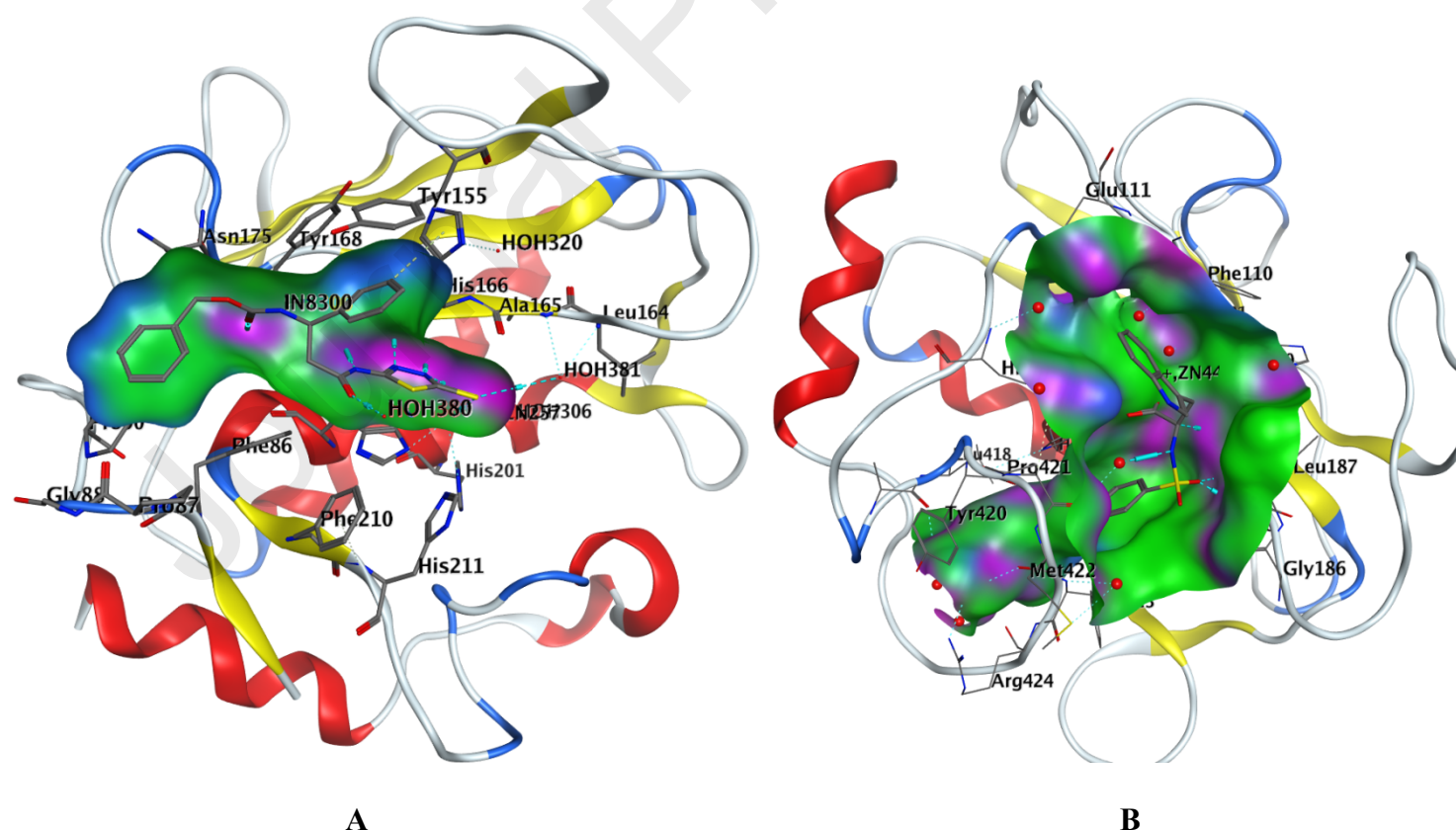


Fig. 2. X-ray structures of **A**) MMP-2 and **B**) MMP-9 with bound inhibitors. Selected amino acids in the active site region and crystallographic water molecules are labeled.

On the basis of the observed interaction patterns and bound inhibitors, we carried out a flexible alignment of the MMP-2/9 inhibitors in (Table 1) in the active sites of MMP-2/9 using the Molecular Operating Environment (MOE) [38] and further refined the alignment through intra- and inter-molecular energy minimization. On the basis of these alignments, a 4-point 3D pharmacophore model for inhibitor binding to MMP-2/9 was derived. (**Fig. 3A**) shows the pharmacophore model that consisted of a hydrophobic/aromatic feature, two hydrogen bond donor functions and a donor/acceptor function

in a defined spatial arrangement [39]. The model represented substructures of inhibitors that formed characteristic interactions or occupied a hydrophobic pocket within in the active site and were considered important for inhibitory activity.

Guided by our structure-based pharmacophore model, we then designed different thiazole-based compounds and examined their detailed fit to the model, which represented the central part of our structure-based design exercise. Compounds derived on the basis of a newly proposed 2-aminothiazole scaffold yielded an excellent fit to the pharmacophore model, as illustrated in (**Fig. 3B**). In exemplary compounds with and without the amidine group, the amidine moiety consistently mapped to the ZBG site represented by the donor/acceptor feature in strongly active compounds and was absent in case of low activity compounds. The excellent fit of the newly designed 2-aminothiazole-based compounds to the pharmacophore model motivated us to synthesize these compounds and test them for MMP-2/9 inhibitory activity.

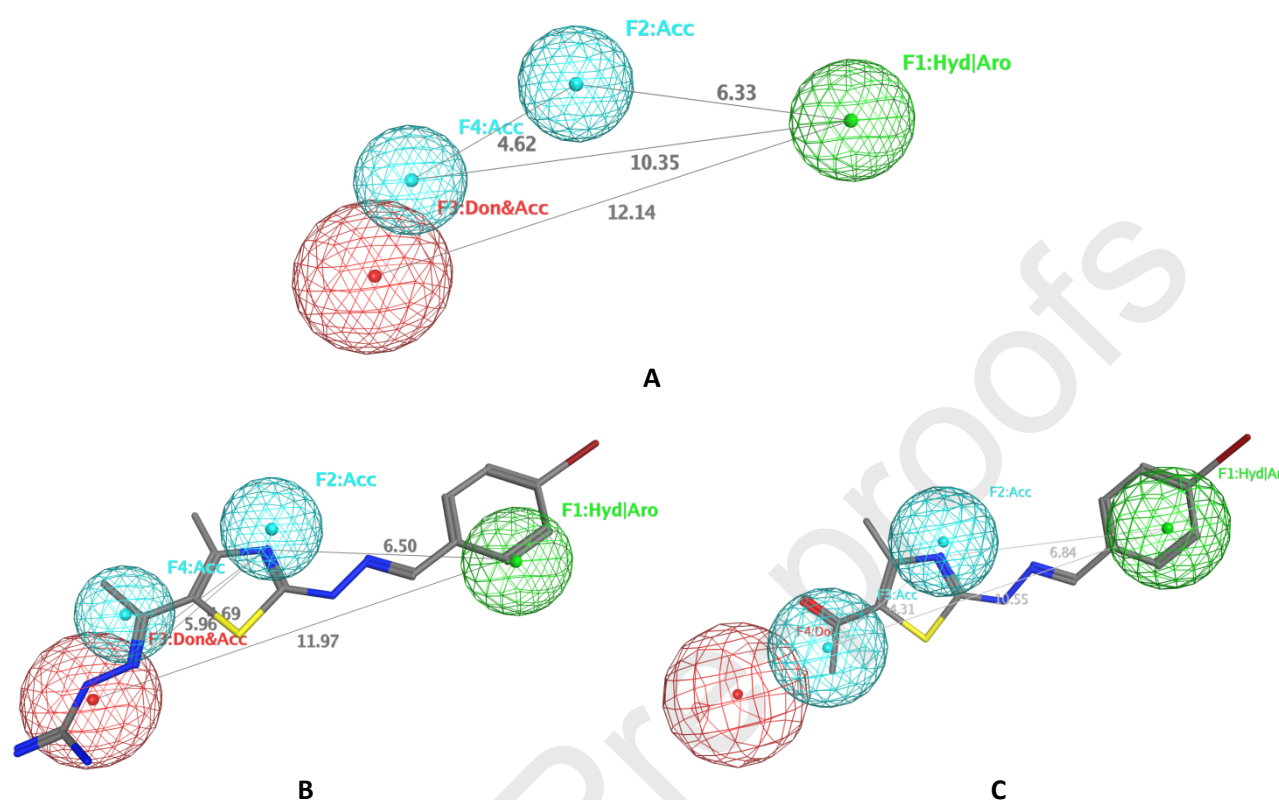
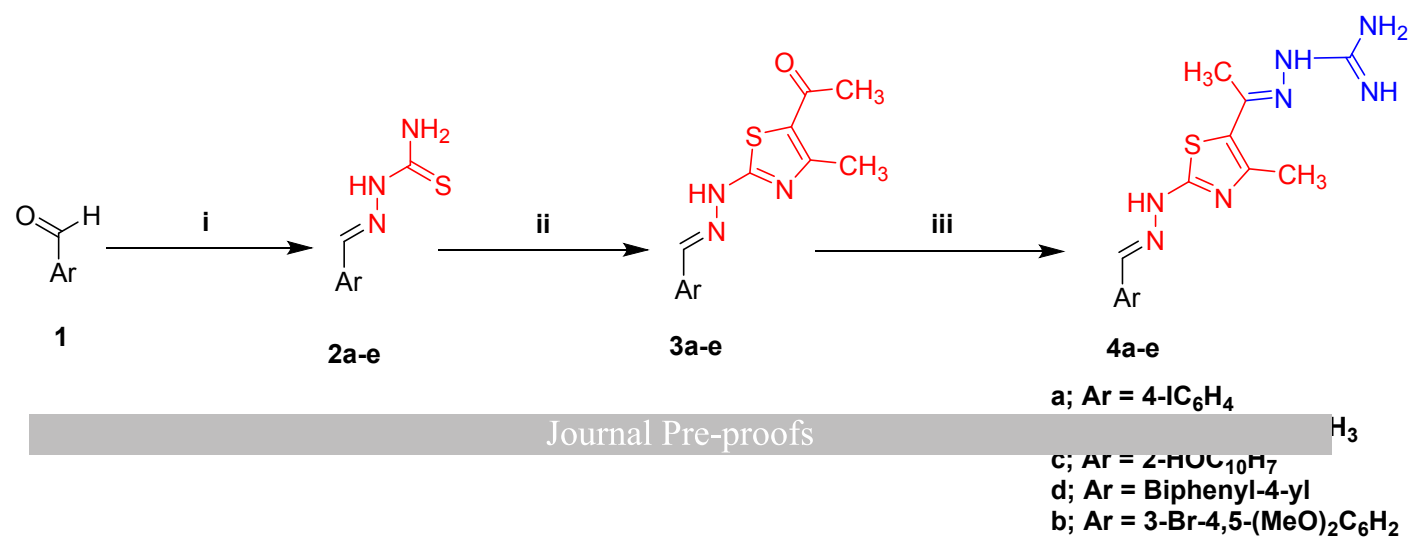


Fig. 3. Pharmacophore model and newly designed inhibitors. **A)** Shows the structure-based 3D pharmacophore model for inhibitor binding to MMP-2/9. Distances between pharmacophore features are given in Å. **B)** Shows the fit of an exemplary Amidine thiazole-based compound to the pharmacophore model. **C)** Shows the fit of an exemplary non-amidine thiazole-based compound to the pharmacophore model.

2.2. Chemistry

Condensation of substituted aromatic aldehydes (**1a-e**), namely 4-iodobenzaldehyde, 4-hydroxy-3-methoxybenzaldehyde, 2-hydroxy-1-naphthaldehyde, [1,1'-biphenyl]-4-carbaldehyde and 3-bromo-4,5-dimethoxybenzaldehyde with hydrazinecarbothioamide in ethanol/AcOH solution under reflux afforded the corresponding 2-arylidenehydrazine-1-carbothioamides (**2a-e**). Cyclization of compounds **2a-e** with 3-chloropentane-2,4-dione in absolute ethanol under reflux gave the cycloaddition products, 1-(2-(2-(arylidenehydrazinyl)-4-methylthiazol-5-yl)ethanone (**3a-e**). Interaction of the later compounds **3a-e** with hydrazinecarboximidamide hydrochloride in absolute ethanol in the presence of a catalytic amount of lithium chloride under reflux for 24 hours resulted in the corresponding 2-(1-(2-((*E*)-2-arylidenehydrazinyl)-4-methylthiazol-5-yl)ethylidene)hydrazinecarboximidamides (**4a-e**). These reactions and the newly designed compounds are depicted in **Scheme 1**. The structure and purity of compounds **2-4** were confirmed by the spectral data as described before [40]. The all characterization data including HNMR, CNMR, LCMS are found in supplementary section in detail.



Scheme 1. Preparation of a series of 4-arylthiazole derivatives (**4a-e**) as novel MMP-2/9 candidate inhibitors and potential anticancer agents. **i**) Thiosemicarbazide/EtOH/AcOH/reflux; **ii**) 3-Chloropentane-2,4-dione/EtOH/reflux; **iii**) Aminoguanidine hydrochloride/EtOH/LiCl/reflux.

2.3. *In vitro* MMP-2/9 inhibitory analysis

We first tested our candidate compounds for MMP-2/9 inhibition in comparison to known MMP-2/9 inhibitors such as NNGH and others [41, 42]. The results are summarized in (Table 2). We found that compound **4a** strongly inhibited MMP-2/9 activity in the lower nanomolar range, with slightly higher potency against MMP-9 (ca. 40 nM). Moreover, compounds **3b**, **3c**, **4d**, and **4e** showed selective inhibition of MMP-9 over MMP-2, with **3b** and **3c** being potent inhibitors of MMP-9. Compound **2c** was after **4a** the overall second strongest inhibitor of MMP-2/9, with comparable potency against both enzymes (in the range of 70-75 nM). The remaining compounds **2a**, **2b**, **2d**, **2e**, **3a**, **3d**, **3e**, **4c** and **4e** were less potent MMP-2/9 inhibitors with potency in the high nanomolar range.

Table 2. *In vitro* inhibitory MMP-2/9 activity of new candidate compounds.

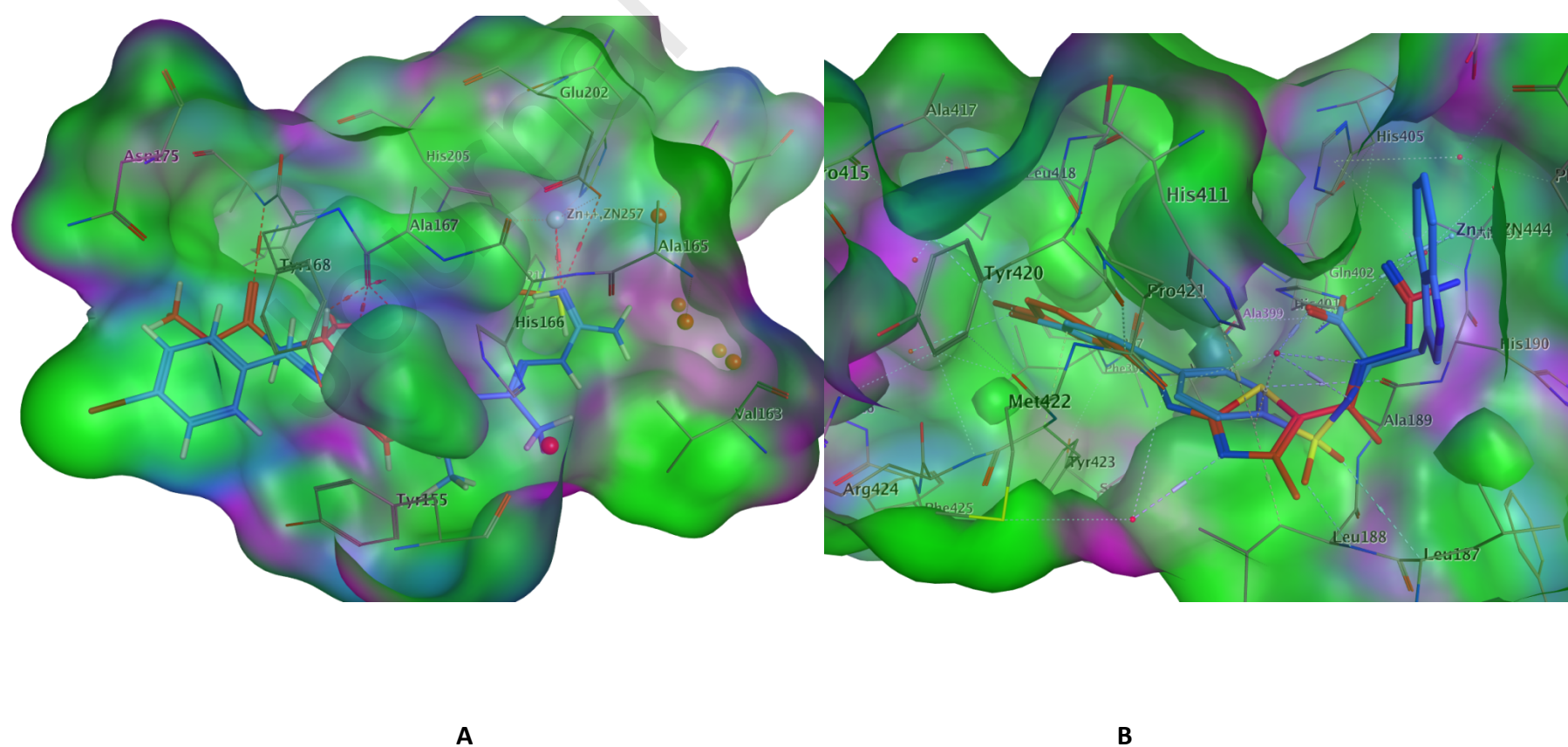
Cpd.	IC ₅₀ (nM)	
	MMP-2	MMP-9
2a	99.53±2.12	590.04±12.6
2b	189.53±4.05	105.82±2.26
2c	71.38±1.52	76.11±1.62
2d	215.18±4.60	94.34±2.01
2e	194.12±4.15	109.17±2.33
3a	472.17±10.1	358.9±7.67
3b	352.04±7.53	20.93±0.44
3c	115.87±2.47	28.77±0.61
3d	237.24±5.07	138.07±2.95
3e	109.82±2.34	137.92±2.95
4a	56.69±1.21	38.60±0.82
4b	98.15±2.10	62.33±1.33
4c	105.86±2.26	86.05±1.84
4d	366.16±7.83	56.87±1.21
4e	149.6±3.20	64.33±1.37
PNU-141803 ^a	310±1.20	49500±0.50
E402Q ^b	9.3 ± 1.5	201.0 ± 58.6
NNGH	39.93±0.85	33.98±0.72

^a Data was taken from ref. [41] and ^bData was taken from ref. [42].
 Data are presented as average IC₅₀ ± SD (nM) values for at least three experiments.

2.4. Molecular docking studies

Having confirmed the MMP-2/9 inhibitory activity of the newly designed compounds, we also investigated putative binding modes of the preferred dual inhibitor **4a** on the basis of docking calculations using MOE [38] and Autodock [43].

From the Protein Data Bank [44] the X-ray structures of MMP-2 in complex with the PNU-141803 inhibitor (PDB entry 2USN) [41] and of MMP-9 in complex with the **E402Q** inhibitor (PDB entry 2OW0) [45] were selected and used as templates for docking. Compound **4a** was built using MOE the geometry was optimized by energy minimization with the CHARMM force field and it was then prepared for docking calculations with Python scripts available in the Autodock package. Prior to docking, bound crystallographic inhibitors were removed from the templates. For re-docking of crystallographic inhibitors and docking of compound **4a**, 50 flexible docking runs were performed using Autodock, and the resulting poses were clustered with 1.8 Å tolerance. Lamarckian genetic algorithm was used for the conformational space search with the initial population set to 150. The most populated clusters of low energy conformations were selected for analysis. For both targets, the applied docking protocol closely reproduced the experimental binding modes of re-docked inhibitors. Furthermore, the predicted binding modes of compound **4a** corresponded to the proposed fit of **4a** to the structure-based pharmacophore model discussed above and to the bound orientation of the crystallographic inhibitors. Specifically, in MMP-2 the guanidine NH of **4a** adopted the formed monodentate interaction with S1' pocket zinc cation consistent with the interactions formed by the reference inhibitors. In addition, as expected, the phenyl moiety of compound **4a** bound to the S1 where it formed aromatic interactions with residues Tyr155 and Tyr168. Furthermore, thiazole ring was accommodated by aromatic interaction with His166. The 2-aminothiazole fragment bound to the S2 subsite of MMP-2/9 where several hydrogen bonding interactions were possible. Corresponding interaction patterns were observed in the docked complex of compound **4a** and MMP-9. The slightly higher potency of **4a** against MMP-9 might be attributable to better shape complementarity and further improved hydrophobic/aromatic interactions within the S1 site compared to MMP-2. (**Fig. 4**) shows the modeled complexes formed by compound **4a** with MMP-2 and MMP-9, respectively. Encouragingly, the results of binding mode predictions for **4a** were fully consistent with pharmacophore fitting as the underlying structure-based inhibitor design strategy. All putative interactions are provided in **Supplementary Table S1, Fig. S1 and Fig. S2**.



2.5. Computational estimation of pharmacokinetic properties

The pkCSM ADMET descriptors algorithm protocol [46-48] was used for calculation of pharmacokinetic (PK) properties such as absorption, distribution, metabolism, excretion and toxicity (ADMET) profiles of compound **4a** and MMP reference inhibitors. (Table 3) summarizes the predicted (computationally estimated) PK profiles of compound **4a** and the reference inhibitors.

Table 3. Predicted ADMET properties of compound **4a** compared to MMP-29 reference inhibitors.

Property	Model Name	Predicted Value		
		4a	PNU-141803	E402Q
Molecular properties	Molecular Weight	441.5	444.5	540.4
	LogP	2.7	3.8	4.4
	Rotatable Bonds	5	7	7
	Acceptors	6	7	3
	Donors	4	3	3
	Surface Area	151.3	171.1	193.1
Absorption	Water solubility	-3.05	-3.53	-4.08
	Caco2 permeability	-0.35	0.262	-0.02
	Intestinal absorption (human)	71.5	81.1	69.8
	Skin Permeability	-2.73	-2.75	-2.73
	P-glycoprotein substrate	Yes	Yes	Yes
	P-glycoprotein I inhibitor	No	Yes	No
	P-glycoprotein II inhibitor	No	Yes	Yes
Distribution	VDss (human)	0.37	0.197	-0.933
	Fraction unbound (human)	0.32	0	0
	BBB permeability	-1.49	-1.23	-1.31
	CNS permeability	-3.72	-2.56	-2.25
Metabolism	CYP2D6 substrate	Yes	No	No
	CYP3A4 substrate	Yes	Yes	Yes
	CYP1A2 inhibitor	No	No	Yes
	CYP2C19 inhibitor	No	Yes	No
	CYP2C9 inhibitor	No	Yes	Yes
	CYP2D6 inhibitor	No	No	No
	CYP3A4 inhibitor	No	Yes	No
Excretion	Total Clearance	0.273	0.064	-0.39
	Renal OCT2 substrate	Yes	No	No
Toxicity	AMES toxicity	Yes	No	Yes
	Max. tolerated dose (human)	0.15	-0.17	0.22
	hERG I inhibitor	No	No	No
	hERG II inhibitor	Yes	No	Yes
	Oral Rat Acute Toxicity (LD50)	2.4	2.4	2.2
	Oral Rat Chronic Toxicity (LOAEL)	1.63	2.25	1.15
	Hepatotoxicity	No	Yes	Yes
	Skin Sensitization	No	No	No
	<i>T.Pyriformis</i> toxicity	0.27	0.43	0.28
	Minnow toxicity	4.59	1.73	0.79

The water/octanol partition coefficient (P) is an important parameter for assessing the hydrophobicity of a compound. The calculated LogP value of **4a** was smaller than for PNU-141803 and E402Q with values of 2.7, 3.8, and 4.4, respectively, indicating that **4a** was less hydrophobic, consistent with the presence of multiple hydrogen bonding donor or acceptor groups. The results for the penetration potential of the blood–brain barrier indicated that compound **4a** and the reference inhibitors had only low potential to cross the barrier, and cause side effects in the central nervous system [48]. The calculated values of the permeability through human skin were -2.73 cm/h **4a**, -2.75 cm/h (PNU-141803), and -2.73 cm/h (E402Q); therefore, the compounds cannot be absorbed through human skin. In the analysis of human intestinal absorption, one of the main parameters for new drug candidates, the analyzed alkaloids had values of 71.5% **4a**, 81.1% (PNU-141803), and 69.8% (E402Q). Some studies [49] have shown that values between 70% and 100% indicate good intestinal absorption. The recommended parameters for the prediction of oral absorption of drugs use Caco-2 permeability models. Calculated values–were 0.35 nm/s **4a**, 0.26 nm/s (PNU-141803), and -0.02 nm/s (E402Q). Furthermore, only PNU-141803 was expected to inhibit P-glycoprotein I, while compounds **4a** was not expected to inhibit P-glycoprotein II a protein responsible for ADME characteristics of different drugs. Cytochrome P450 (CYP) profiling calculations indicated that **4a** was unable to inhibit CYP 2C19, CYP 2D6, and CYP 3A4, increasing the ability

of these proteins to metabolize other drugs in the body and lowering the probability of serious adverse effects. However, PNU-141803 and E402Q) were inhibit of CYP 2C19, CYP 2C9, and CYP 3A4, reducing the ability of these proteins to metabolize other drugs in the body. Compound **4a** was also predicted not to inhibit CYPAD6. The parameter total clearance is related to bioavailability and is important in determining dosage rates to achieve steady state concentration Calculated values of **4a** was higher than of the references. Thus, these compounds, due to their high hydrophilicity, could be excreted rapidly by the kidneys, requiring shorter administration intervals to maintain desired therapeutic concentrations. The last parameter analyzed in our studies was hepatotoxicity, compound **4a** was indicated to have AMES toxicity but had lower oral rat chronic toxicity (LOAEL) than the reference inhibitors and was not indicated to have hepatotoxic effects indicating the absence of potential hepatic injury and the presence of liver tolerance. Taken together, the results of computational PK parameter profiling indicated that compound **4a** had favorable ADMET properties at least comparable to, if not better than the reference inhibitors.

2.6. Anticancer assay

Anti-proliferative activity of the synthesized compounds **2a-e**, **3a-e** and **4a-e** was examined on three human cancer cell lines, namely, invasive breast cancer cell line (MDA-MB-231), human colon cancer (HCT-116) and mammary gland breast cancer (MCF-7). In addition, the two normal cell lineshuman keratinocytes cell line (HaCaT) and human diploid fibroblasts (WI-38) were investigated as controls. *In-vitro* cytotoxicity evaluation using a viability assay [50,51] was performed with staurosporine as a cytotoxic reference compound. The results were expressed as growth inhibitory concentration (IC_{50}) values which represent the compound concentrations required to produce a 50% inhibition of cell growth after 24 h of incubation as shown in (Fig. 5) and (Table 4).

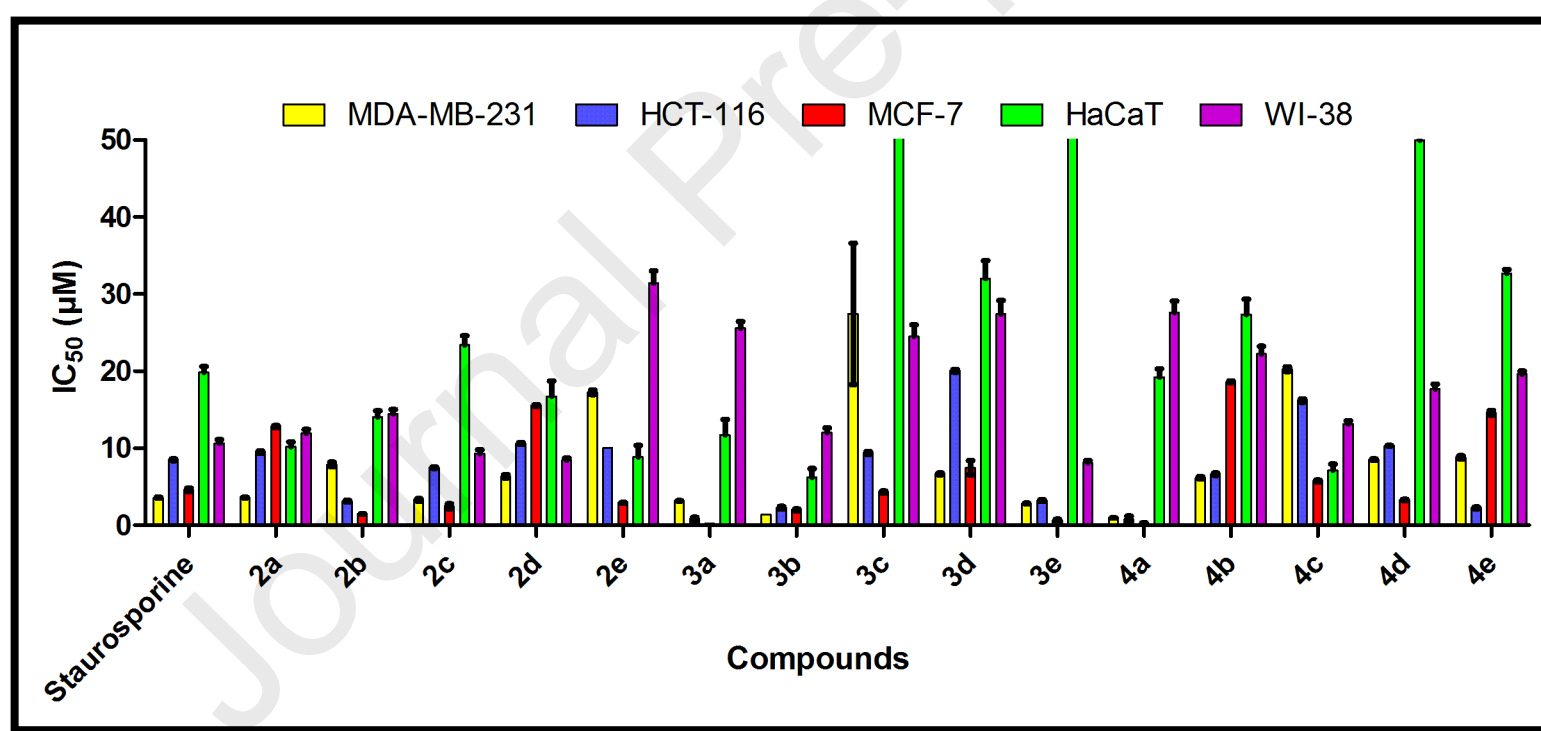


Fig. 5. IC_{50} (μ M) of the target compounds against MDA-MB-231, HCT-116, MCF-7 tumor cells and HaCaT, WI-38 normal cell lines.

Table 4. Cytotoxic activity of the target compounds against different cell lines.

Cpu.	Ar	Journal Pre-proofs				
		Cancerotoxicity			Normotoxicity	
		MDA-MB-231	HCT-116	MCF-7	HaCaT	WI-38
2a	4-IC ₆ H ₄	3.06±0.09	9.5±0.12	12.82±2.1	10.20±0.66	11.94±0.74
2b	4-HO-3-MeOC ₆ H ₃	7.89±0.31	3.12±0.16	1.46±1.6	14.06±0.81	14.42±1.03
2c	2-HOC ₁₀ H ₇	3.30±0.13	7.48±2.30	2.46±0.44	23.39±0.78	9.30±0.44
2d	Biphenyl-4-yl	6.35±0.33	10.61±0.11	15.56±1.5	16.72±0.71	8.43±0.43
2e	3-Br-4,5-(MeO) ₂ C ₆ H ₂	17.26±0.82	10.02±0.23	2.92±1.3	8.86±0.39	31.43±1.87
3a	4-IC ₆ H ₄	3.18±0.22	0.84±1.4	0.23±1.5	11.71±1.37	25.55±1.46
3b	4-HO-3-MeOC ₆ H ₃	1.35±0.04	2.26±2.5	2.01±2.1	6.24±0.43	12.04±0.81
3c	2-HOC ₁₀ H ₇	27.44±9.76	9.38±11.2	4.31±10.2	69.98±2.22	24.54±1.62
3d	Biphenyl-4-yl	6.65±0.24	26.06±1.3	7.49±3.1	32.04±1.91	27.38±1.55
3e	3-Br-4,5-(MeO) ₂ C ₆ H ₂	2.83±0.09	3.26±2.1	0.66±1.4	61.14±2.69	8.11±0.33
4a	4-IC ₆ H ₄	0.97±0.03	0.77±0.05	0.02±2.2	19.21±0.88	27.61±1.62
4b	4-HO-3-MeOC ₆ H ₃	6.16±0.51	6.62±0.32	18.62±3.1	27.34±1.14	22.23±1.08
4c	2-HOC ₁₀ H ₇	20.28±1.31	16.19±2.1	5.75±14.2	7.15±0.34	13.16±0.76
4d	Biphenyl-4-yl	8.53±0.41	10.33±4.2	3.29±2.1	49.97±2.17	17.70±0.64
4e	3-Br-4,5-(MeO) ₂ C ₆ H ₂	8.80±0.26	2.25±10.2	14.60±4.1	32.69±1.79	19.60±0.69
Staurosporine	-	3.57±0.07	8.5±0.11	4.6±0.21	19.85±0.75	10.63±0.47

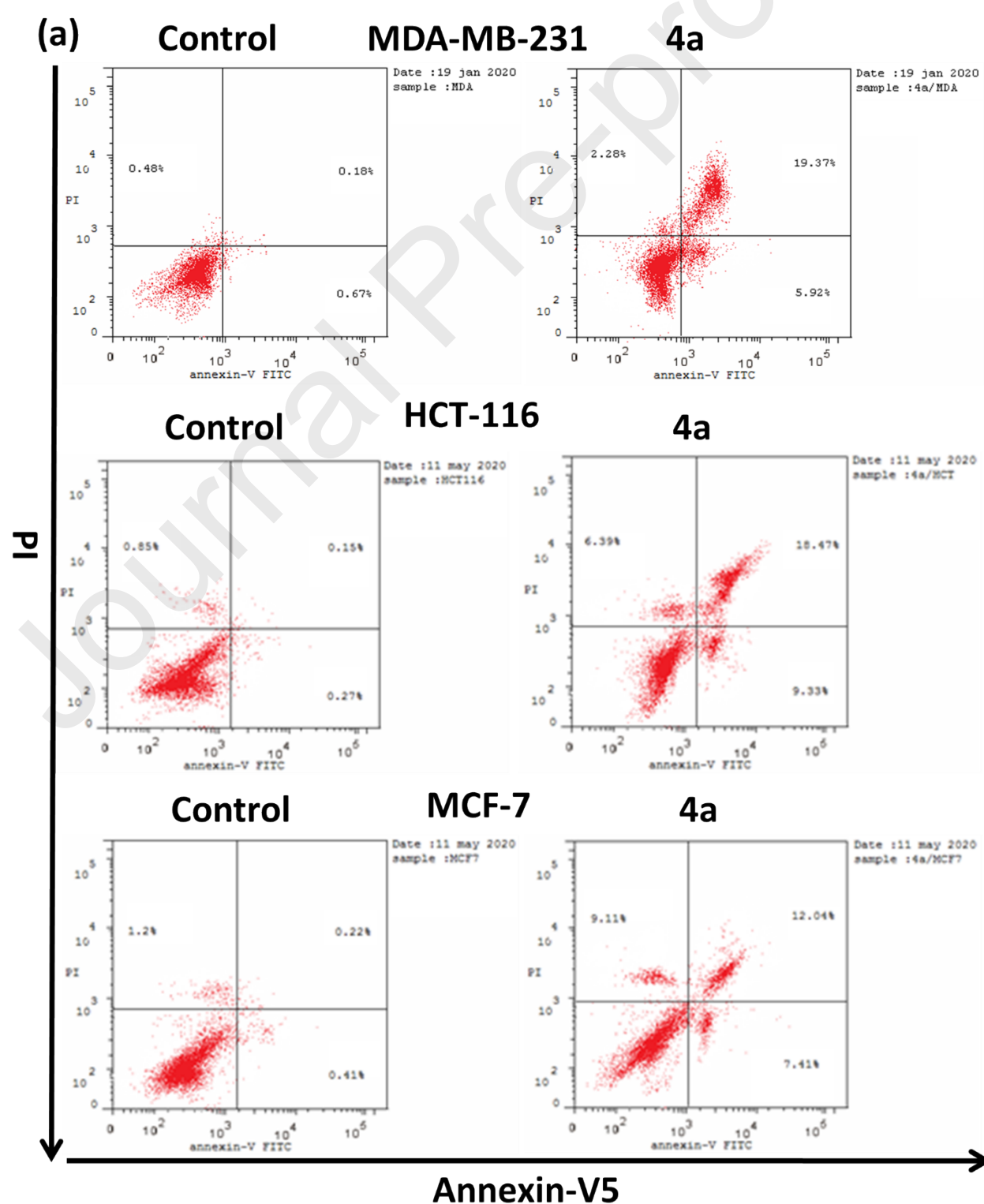
^a IC₅₀ values expressed in μ M as the mean values of triplicate wells from at least three experiments and are reported as the mean \pm standard error.

From Table 1, it was noticeable that staurosporine had an IC₅₀ of 3.57–8.50 μ M and 10.63-19.85 μ M against all the cell lines that were investigated with a differentiation between cancer and normal cells. In addition, some of the new compounds displayed an excellent to modest growth inhibitory activity against the tested cancer cell lines and were active or inactive against normal cell lines, HaCaT and WI-38. Compounds **2a** and **2c** were the most potent derivatives against cancer cell lines such as MDA-MB-231 with IC₅₀ 3.06±0.09 and 3.30±0.13 μ M, respectively, as compared to the standard staurosporine (IC₅₀, 3.57±0.07 μ M) Compounds **2b** and **2c** also showed cytotoxic activity against cancer cell lines HCT-116 and MCF-7 with IC₅₀ (3.12±0.16, 1.46±1.6 and 7.48±2.30, 2.46±0.44 μ M), respectively, as compared to staurosporine (IC₅₀, 8.5±0.11 and 4.6±0.21 μ M) Compound **2e** possessed excellent antiproliferative activity against MCF-7 with IC₅₀ 2.92±1.3 μ M. Compounds **2a-e** were moderately active or nearly inactive against the cell lines HaCaT and WI-38 with IC₅₀ ranging from 8.43-31.43 μ M compared to Staurosporine (IC₅₀, 19.85±0.75 and 10.63±0.47 μ M, respectively. Additionally, compounds **3a,b,e** with IC₅₀ = 1.35-3.8, 0.84-3.26 and 0.23-2.01 μ M, respectively, possessed excellent antiproliferative activities against all cancer cell lines MDA-MB-231, HCT-116, and MCF-7, which was superior to Staurosporine with IC₅₀, 3.57±0.07, 8.5±0.11 and 4.6±0.21 μ M, respectively. Compounds **3a-e** displayed a growth inhibitory activity against normal cell lines HaCaT and WI-38 with IC₅₀ ranging from 8.11-69.98 μ M. Furthermore, compounds **4a** had superior potency against all the cancer cell lines MDA-MB-231 HCT-116 and MCF-7 with IC₅₀ 0.97±0.03, 0.77±0.05 and 0.02±2.2 μ M, respectively, compared to Staurosporine. Compounds **4e,b** also exhibited strong cytotoxic activity against the cancer cell line HCT-116 with IC₅₀ 2.25±10.2 and 6.62±0.32 μ M, respectively, while compounds **4d,c** displayed less anti-proliferative activities than Staurosporine with IC₅₀ values of 3.29±2.1 and 5.75±14.2 μ M, respectively. Finally, compounds **4a-e** had growth inhibitory activity against HaCaT and

WI-38 with IC_{50} ranging from 7.15-49.97 μ M. In particular, **4a** was only weakly active against these control cell lines, with strong selectivity in antiproliferative effects for the cancer lines.

2.7. Cell apoptosis

Annexin V binding to phosphatidylserine (PS) exposed on the external leaflet of the plasma membrane during apoptosis is widely accepted as an indicator of apoptotic Journal Pre-proofs induced by compound **4a** treatment was related to apoptosis, we determined apoptosis using the Annexin/PI double staining flow cytometric assay (**Fig. 6a**). The percentage of total apoptotic cells (early and late apoptotic cells) increased from about 2% for the control to about 30% in the case of all tested cancer cells treated with compound **4a**. These results showed that compound **4a** induced apoptosis at a similarly higher rate in MDA-MB-231, HCT-116, and MCF-7 cancer cells (**Fig. 6b**). Necrosis cell death leads to the release of the intracellular contents that affects neighboring cells and triggers an inflammatory reaction [53]. However, we did not observe cells undergoing necrosis upon treatment with compound **4a**, indicating that cell death occurred primarily through apoptosis. In cancer therapy, most efficient and safe anticancer agents typically interfere with the balance between cell proliferation and apoptosis and shift cells toward the induction of apoptosis [54]. Our findings are consistent with other studies showing that MMPiS inhibit tumor proliferation by inducing apoptosis [55,56], as clearly detected for compound **4a**.



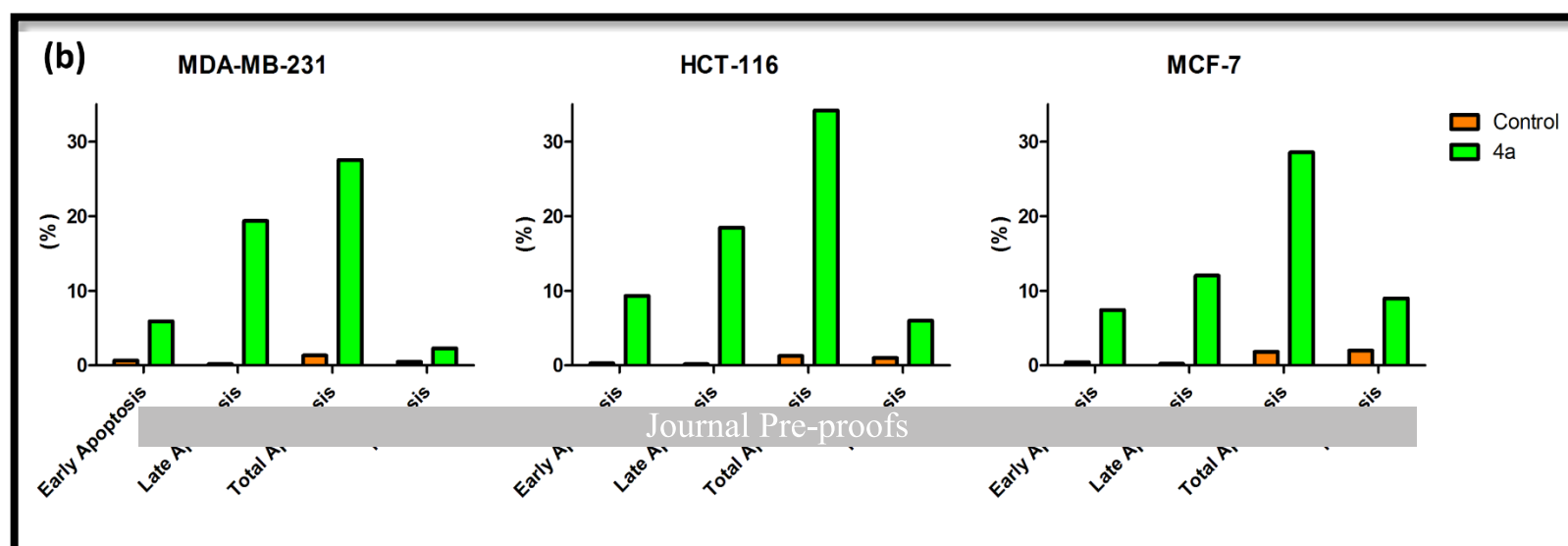


Figure 6: (a) Dot plot of Annexin V/PI double staining of control and treated cells. (b) Statistical analysis of the apoptosis percentage of MDA-MB-231, HCT-116, and MCF-7 cells after incubation with compound **4a** for 24 h (IC_{50} value). The data are reported as the mean \pm SD of three independent experiments in triplicate.

2.8. DNA fragmentation

DNA fragmentation is the characteristic event common to all processes of apoptosis [57]. Diphenylamine assay was used to determine the percentage of fragmented DNA released from apoptotic nuclei into the cytoplasm. The relative quantity of DNA fragments in the MDA-MB-231, HCT-116, and MCF-7 cells treated with compound **4a** is shown in (Fig. 7). The percentage of DNA fragmentation increased significantly in all cells treated with compound **4a** (about 30%) compared to untreated control (about 5%), without significant differences observed between tested cells. These results were consistent with the apoptosis results discussed above suggesting that treatment of MDA-MB-231, HCT-116, and MCF-7 cells with compound **4a** induced cell membrane disruption followed by fragmentation of chromosomal DNA.

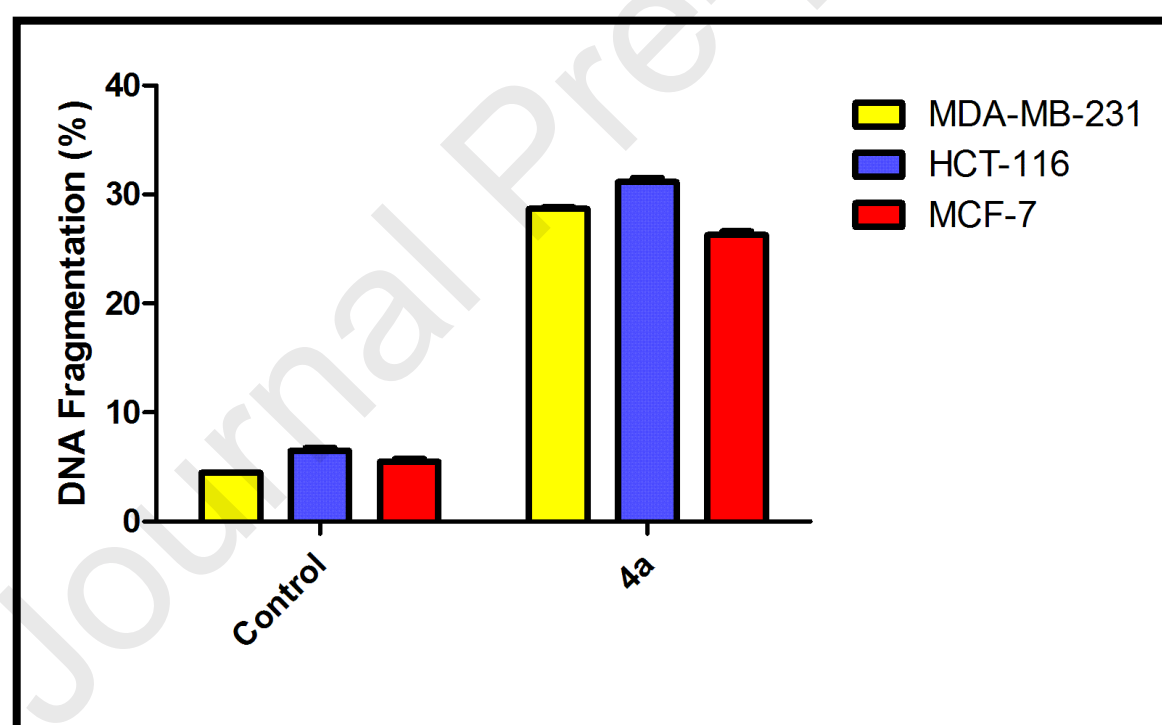


Fig. 7: Statistical analysis of the DNA fragmentation percentage of MDA-MB-231, HCT-116, and MCF-7 cells after incubation with compound **4a** for 24 h (IC_{50} value). The data are reported as the mean \pm SD of three independent experiments in triplicate.

2.9. Cell cycle analysis

For the reduction of possible nonspecific drug effects in cancer treatment, the design and synthesis of novel chemotherapeutic agents that can regulate cell cycle progression and apoptosis is an attractive approach [58]. Therefore, further effects of compound **4a** on regulating cell cycle progression were explored using the Propidium Iodide Flow Cytometry Kit assay (Fig. 8a). The percentages of compound **4a** treated MDA-MB-231, HCT-116, and MCF-7 cells in the G2/M phase were significantly higher than those in the control group. Moreover, the distribution of cells in the G1 and S phases was notably decreased in all tested cells compared to the control (Fig. 8b). Previous studies showed that MMPs aligned along the microtubular network within the cells during the mitotic phase. In addition, intracellular MMP-2/9 inhibitors have been associated with antimitotic action [59,60]. This might provide a possible explanation of cell cycle arrest observed at G2/M phase in cells treated with compound **4a**.

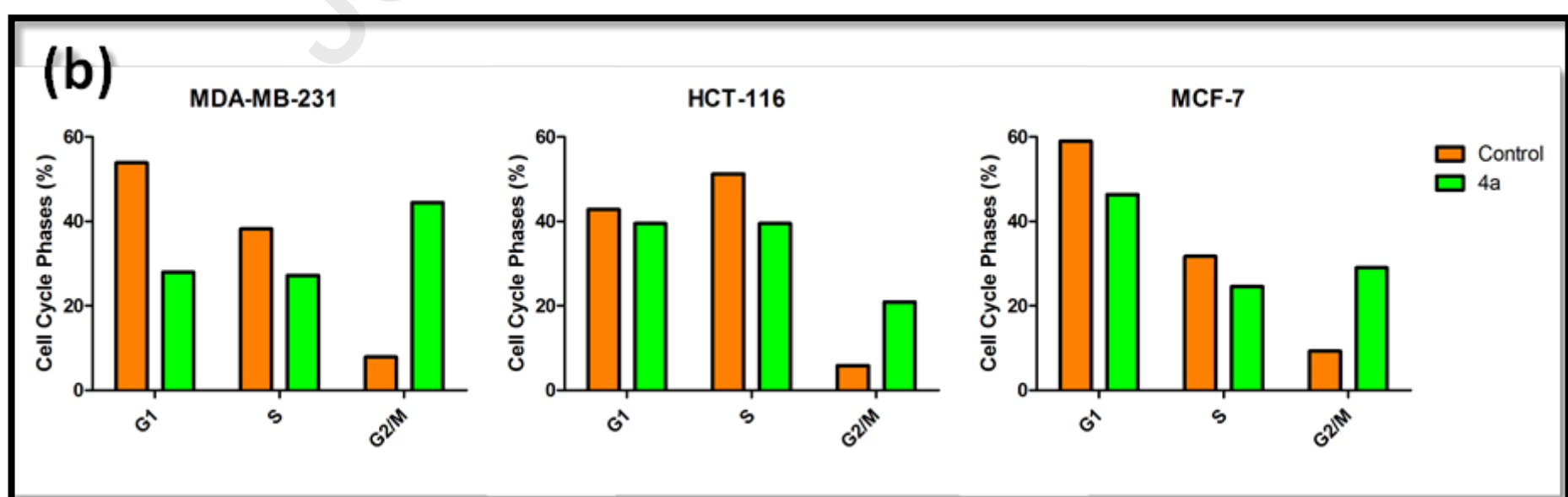
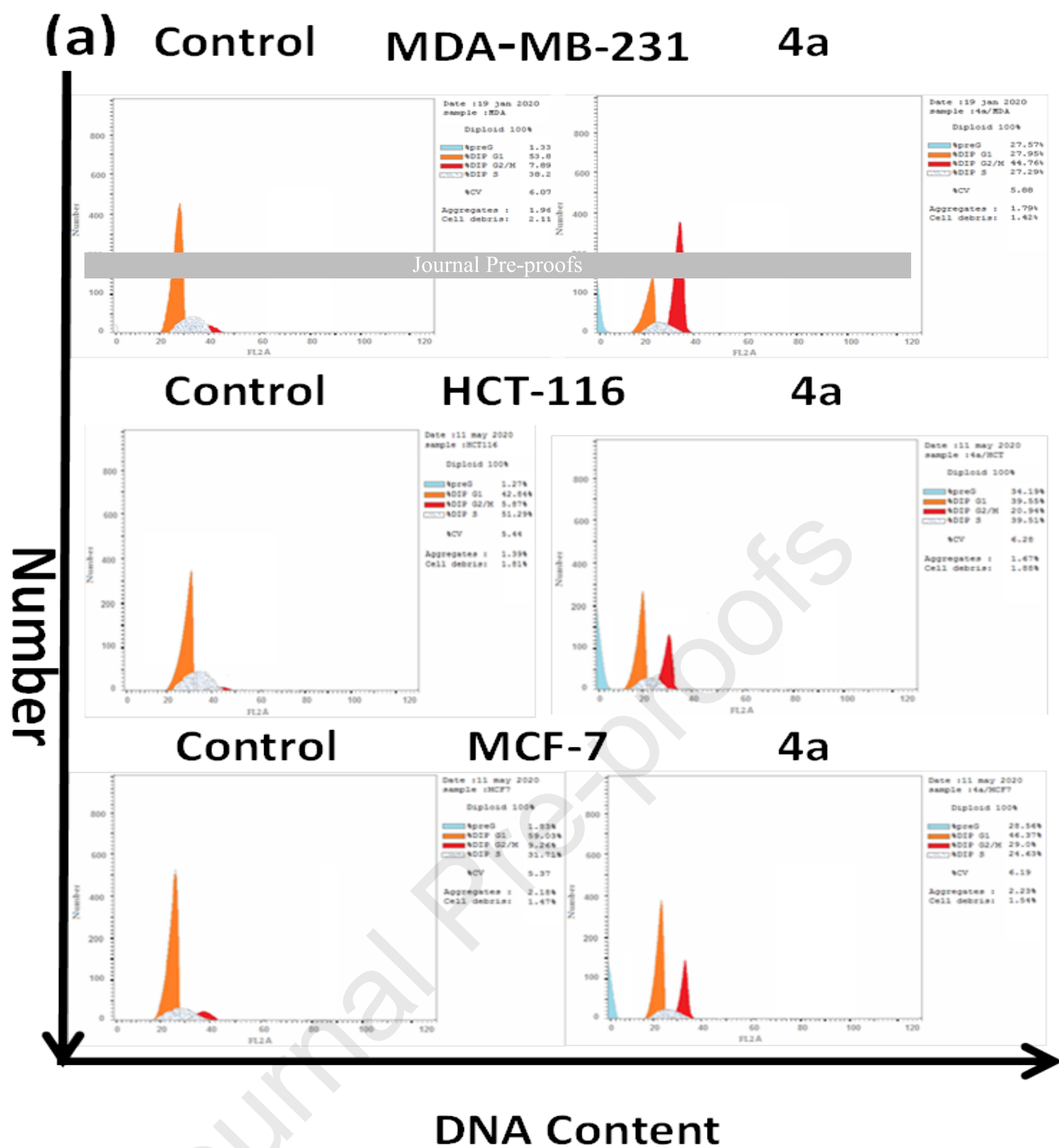
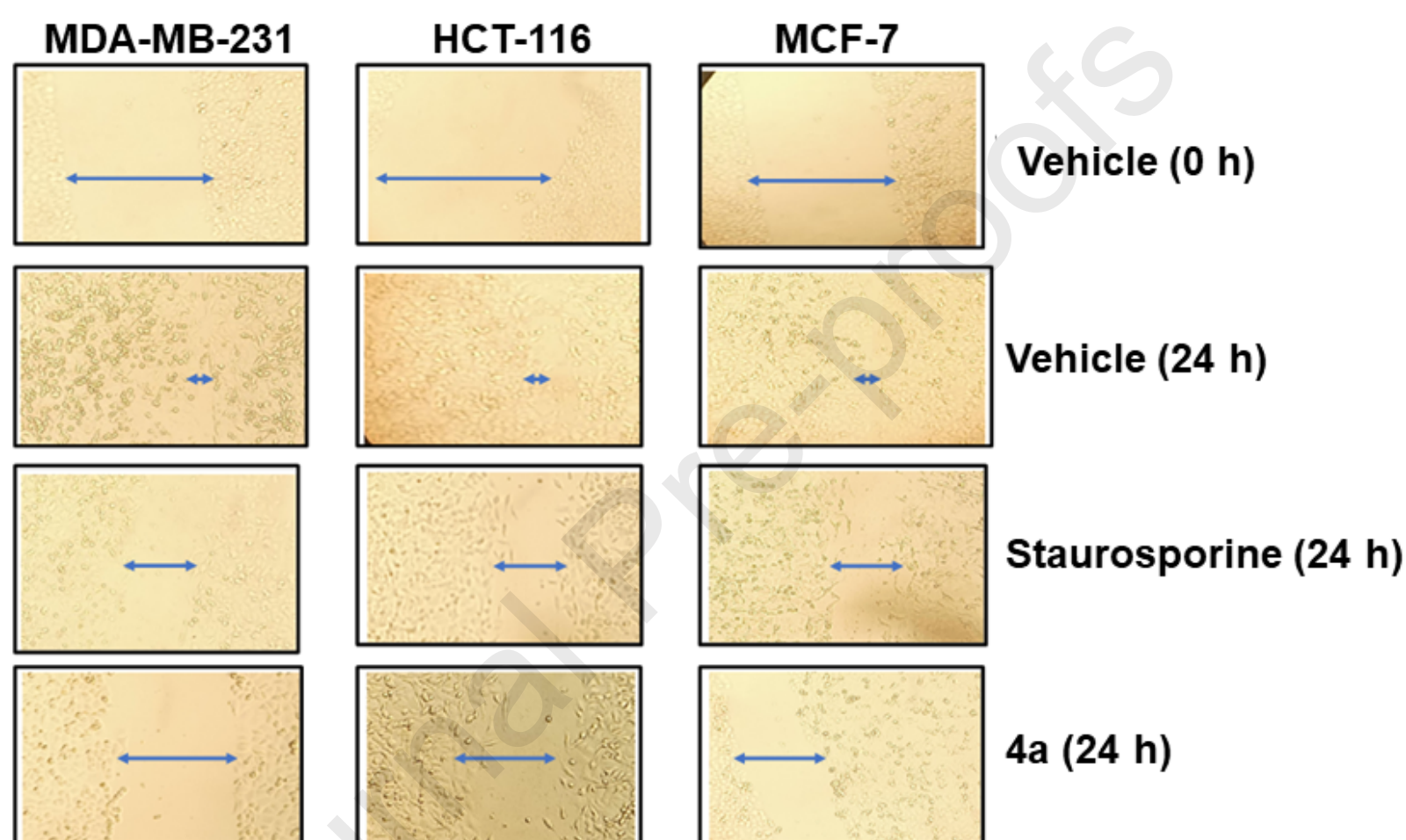


Fig. 8: (a) DNA content distribution histograms of control and treated cells. (b) Statistical analysis of cell cycle phases percentage of MDA-MB-231, HCT-116, and MCF-7 cells after incubation with compounds **4a** for 24 h (IC₅₀ value). The data are reported as the mean \pm SD of three independent experiments in triplicate.

2.10. Wound healing assay

Controlled proteolysis is required for cell migration across and through tissues in wound healing, tumor growth, and metastasis. Several MMPs were prominently expressed in wound healing and migration of tumor cells within the surrounding matrix environment [61]. Furthermore, in a culture-dependent gelatinase secretion profile, higher expression levels of MMP-2 and MMP-9 were observed in both spheroids and monolayer cultures of MDA-MB-231 cells [62]. In this study, the observed cell cycle arrest at the G2/M phases raised the possibility that compound **4a** might manipulate cell migration. Therefore, a wound healing assay (see Experimental Section) was used to determine possible effects of compound **4a** on the migratory capacity of MDA-MB-231, HCT-116, and MCF-7 cells (**Fig. 9a**). Compound **4a** induced a substantial decrease in the wound closure percentage in all the tested cells compared to untreated control cells (**Fig. 9b**). This result is consistent with another study also showing the inhibitory effect of triazole derivatives on metastatic cancer cell migration and invasion [63]. Indeed, the inhibitory effect of compound **4a** on MMP-2/9 reduced the migration potential of the MDA-MB-231, HCT-116, and MCF-7 cancer cell lines.

a)



b)

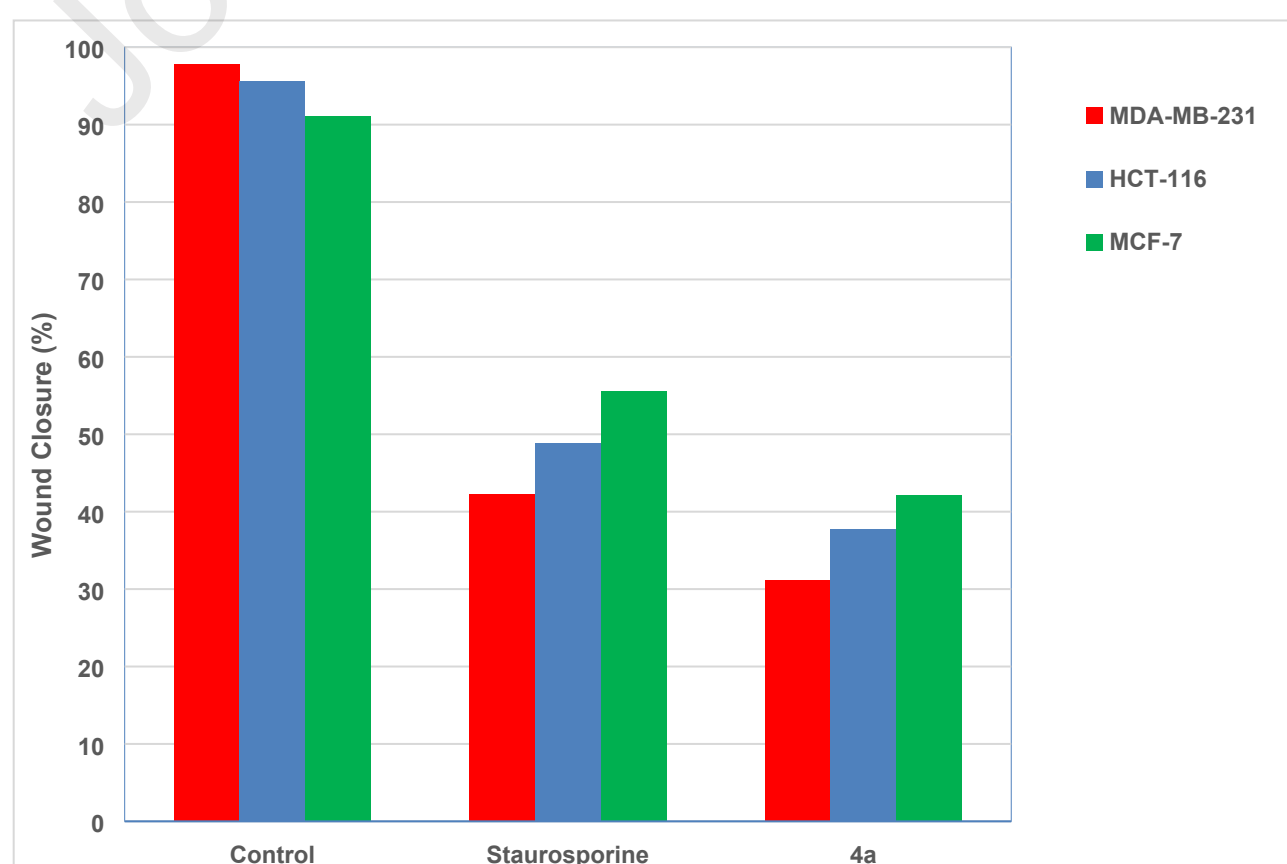


Fig. 9: (a) MDA-MB-231, HCT-116, and MCF-7 cultured cells confluence in 24-well culture plates containing an insert that forms a 0.9 mm gap on the monolayer (Vehicle control at 0 h.). After the insert was removed, untreated cells (Vehicle control at 24 h) and cells treated with staurosporine or compound **4a** for 24 h were imaged under an inverted light microscope. Arrows are pointing toward wound edges. (b) Statistical analysis of wound closure percentage of MDA-MB-231, HCT-116, and MCF-7 cells after incubation with compound **4a** for 24 h (IC₅₀ value).

2.11. Structure-activity relationship studies

The structure-activity relationship (SAR) study revealed that the antitumor activity of the three series **2a-e**, **3a-e** and **4a-e** was significantly affected by the hydrophobic vs. hydrophilic nature of the substituents. In a comparison of the cytotoxic activities of the three series (**2a-e**, **3a-e** and **4a-e**) against invasive breast, colon and breast cancer, we found that varying the substitution patterns of the phenyl, naphthyl, and biphenyl rings at the 2-position of the hydrazine carbothioamide moiety, compounds **2a** and **2c** (first series) revealed significant impact on the activities against the MDA-MB-231 cell line compared to staurosporine where the activities were decreased in the order of 4-I > 2-OH > Ph-4-Ph > 4-HO-3-MeO > 3-Br-4,5-(MeO)₂. These observations suggested that modifying the phenyl or naphthyl ring with small hydrophobic (iodo atom) or hydrophilic (hydroxyl group) substituents was more beneficial than other substitutions. With respect to the activity against the HCT-116 and in particular MCF-7 cell line, molecules **2b**, **2c** and **2e** were the most effective analogues generated in this study compared to staurosporine. These findings also indicated that the combination of hydrophilic and hydrophobic (hydroxyl and methoxy groups) or hydrophilic (hydroxyl group) and hydrophobic (bromo atom and two methoxy groups) substituents resulted in excellent antiproliferative activities. Further investigation of the impact of the substitution pattern of the aryl moiety in the thiazole derivatives **3a-e** (second series) against the cancer cell lines MDA-MB-231, HCT-116 and MCF-7 was carried out. Incorporation of iodo atom, hydroxyl and methoxy groups or bromo atom and two methoxy groups on the phenyl moiety rendered compounds **3a**, **3b** and **3e** highly cytotoxic against the three tumor cell types, implying that the presence of small hydrophobic or hydrophilic (iodo, bromo atoms or methoxy and hydroxyl groups) substituent was indispensable for the activities against cancer cell lines. Furthermore, the assessment of the substitutions at the previous positions of the aryl group on the thiazolyl hydrazinecarboximidamide system (**4a-e**) (third series) for activity against the cancer cell lines MDA-MB-231, HCT-116 and MCF-7 revealed that compounds **4a** showed high activity against all cancer cell lines. These findings suggested that grafting of a hydrophobic substituent such as the iodo atom on the phenyl ring was more favorable than the other the substituents, while introduction of a hydroxyl and methoxy group or bromo atom and two methoxy groups on the phenyl moiety of compounds **4b** and **4e** and hydroxyl or biphenyl groups for compounds **4c** and **4d** resulted in an increase in activity against cancer cell lines, HCT-116 and MCF-7, respectively. It follows that the substitution pattern on the aryl moiety was a crucial element of the antitumor activity. The incorporation of hydrophobic and/or hydrophilic groups greatly enhanced the activity. Finally, the order of anticancer activities of the three series was decreased in the order of **4a-e** > **3a-e** > **2a-e**.

3. Concluding remarks

Many of pathological disorders like cancer invasion, metastasis, and angiogenesis, as well as cardiovascular, neurologic and inflammatory diseases are linked to expressing a lot of metalloproteinases like MMP2/9 [64-66]. Accordingly, MMP expression is tied to tumor progression, stages, and patient prognosis [67]. These MMPs are also involved in processes and signaling pathways implicated in angiogenesis, cell migration and invasion, and other cellular functions such as proliferation, apoptosis, and differentiation [68]. Accordingly, MMP-2/9 is attractive targets for cancer therapy development. In this study, a series of 4-aminothiazole compounds containing lipophilic aromatic and guanidine termini have been designed, synthesized and evaluated for dual MMP-2/9 inhibitory activity. Most of the synthesized derivatives had comparable of higher activity than reference inhibitors. Compound **4a** was the most potent MMP-2/9 inhibitor with IC₅₀ values of 56 nM and 38 nM, respectively. We also evaluated anti-proliferative activities of the new compounds against MDA-MB-231, HCT-116, and MCF-7 cells compared to two normal cell lines HaCaT and WI-38. Most of the compounds exhibited higher antiproliferative activities than a positive control drug. In addition, compound **4a** promoted apoptosis of MDA-MB-231, HCT-116, and MCF-7 cells, induced cell cycle arrest at the G2/M phase, inhibited the invasion and migration and induced DNA fragmentation in MDA-MB-231, HCT-116,

and MCF-7 cancer cells. Based on our results, compound **4a** is indicated to have considerable potential as a new amidine-based lead compound for the discovery of new anticancer agents targeting MMP-2/9 enzymes. We plan on continuing optimize efforts on this compound to obtain chemical entities with highly anticancer activity.

4. Experimental section

4.1. General chemistry

The starting reagents and solvents were purchased from the Aldrich Company and were used as received. Melting points (Mp) were determined in open capillary tubes using electrothermal apparatus (Stuart, UK) and are uncorrected. The IR spectra were recorded on a KBr disc on a Shimadzu 8201 PC, FTIR spectrophotometer (ν_{max} in cm^{-1}). All the new compounds were characterized by the ^1H -NMR and ^{13}C -NMR, using a ^1H -NMR (400 MHz) and ^{13}C -NMR (100 MHz) spectra, and were measured in DMSO at room temperature. The chemical shifts (δ) were reported in ppm to a scale calibrated for tetramethylsilane (TMS), which is used as an internal standard. HPLC-Mass Spectrometry was performed on Agilent 1100 / ZQ MSD including C18 column and diod-array UV detector. The mobile phase (containing 0.01 M ammonium acetate) was gradient starting from 20% acetonitrile/80% water to 80% acetonitrile/20% water. Purities are reported according to percentage of Peak Areas at wavelength 254 nm. Biological activities were carried out at the Regional Centre for Mycology & Biotechnology, Al-Azhar University, Cairo, Egypt. The follow up of the reactions and the check of the purity of the compounds were made by the TLC on silica gel-protected aluminum sheets (Type 60 GF₂₅₄, Merck), and the spots were detected by exposure to a UV-lamp at λ 254 nm for a few seconds.

4.1.1. General procedure for the synthesis of substituted 2-arylidenehydrazine-1-carbothioamides (2a-e)

2-Arylidenehydrazine-1-carbothioamides were prepared according to previous reported procedure [40].

4.1.2. General procedure for the synthesis of substituted 1-(2-(2-arylidenehydrazineyl)-4-methylthiazol-5-yl)ethanones (3a-e)

1-(2-(2-(Arylidenehydrazinyl)-4-methylthiazol-5-yl)ethanone (**3a-e**) were prepared according to previous reported procedure [40].

4.1.3. General procedure for the synthesis of substituted 2-(1-(2-(2-(4-benzylidene)hydrazinyl)-4-methylthiazol-5-yl)ethylidene)-hydrazinecarboximidamides (4a-e)

2-(1-(2-(2-(4-arylidene)hydrazinyl)-4-methylthiazol-5-yl)ethylidene)hydrazinecarboximidamides (**4a-e**) were prepared according to previous reported procedure [40].

4.2. MMP Enzyme inhibition assay

Screening for MMP-2 (EC 3.4.24.35) inhibitors was performed using the MMP-2 Inhibitor Screening Kit (Fluorometric) (BioVision, Milpitas, CA 95035 USA, Catalog # K2017-100, <https://www.biovision.com/>) and MMP-9 assay was performed using abcam139448 kit MMP9 Inhibitor Screening Assay Kit (Colorimetric) (abcam, Catalog # ab139448, <https://www.abcam.com/>) according to the manufacturer's guidelines.

4.3. Cytotoxicity evaluation using a viability assay

The cytotoxic activity was assessed using the 3-(4,5-dimethylthiazol-2-yl)-2,5-diphenyl tetrazolium bromide (MTT) colorimetric assay as reported previously [50,51].

4.4. Quantification of apoptosis by flow cytometry

Annexin V-FITC apoptosis assay was performed by using Annexin V-FITC/PI double staining detection kit (BD Pharmingen, USA).[69, 70] Flow cytometric analysis was performed on FACS Calibur flow cytometer (BD Biosciences, Franklin Lakes, NJ, USA). Annexin V-FITC was detected

through (FL1) channel while PI was detected through the (FL2) channel. Finally, a minimum of 10,000 cells per sample were acquired and analyzed using Cell Quest Pro software (BD Biosciences).

4.5. DNA fragmentation

DNA fragmentation was quantitatively determined using diphenylamine (DPA) reagent according to the method of Boraschi and Maurizi.[71-73]

4.6. Cell cycle analysis

Cell cycle arrest and Journal Pre-proofs followed by flow cytometry analysis. The DNA content in each cell nucleus was determined by a FACS Calibur flow cytometer (BD Biosciences, Franklin Lakes, NJ, USA). Finally, cell cycle phase distribution was analyzed using Cell Quest Pro software (BD Biosciences) showing collected propidium iodide fluorescence intensity on FL2 [74].

4.7. Wound healing assay

Cancer cell migration was assessed using a wound healing assay (CytoSelect™ Wound Healing Assay Ki. Cell Biolabs, Inc. San Jose) as previously reported [75,76]. Cells were imaged under an inverted light microscope (Nikon Eclipse Ti and NIS-Elements software).

Acknowledgment

This project was funded by the Deanship of Scientific Research (DSR), King Abdul-Aziz University, Jeddah, under grant No. (RG-8-166-38).

References

- [1] S.F. Sener, N. Grey, The global burden of cancer, *Journal of surgical oncology*, 92(1) (2005) 1-3.
- [2] E. Salminen, J. Izewska, P. Andreo, IAEA's role in the global management of cancer-focus on upgrading radiotherapy services, *Acta oncologica* (Stockholm, Sweden), 44(8) (2005) 816-24.
- [3] L.A. Garraway, P.A. Janne, Circumventing cancer drug resistance in the era of personalized medicine, *Cancer discovery*, 2(3) (2012) 214-26.
- [4] L. Denny, The prevention of cervical cancer in developing countries, *BJOG : an international journal of obstetrics and gynaecology*, 112(9) (2005) 1204-12.
- [5] J. Ferlay, I. Soerjomataram, R. Dikshit, S. Eser, C. Mathers, M. Rebelo, D.M. Parkin, D. Forman, F. Bray, Cancer incidence and mortality worldwide: sources, methods and major patterns in GLOBOCAN 2012, *International journal of cancer*, 136(5) (2015) E359-86.
- [6] P.A. Konstantinopoulos, A.G. Papavassiliou, Seeing the future of cancer-associated transcription factor drug targets, *Jama*, 305(22) (2011) 2349-50.
- [7] T.A. Chohan, A. Qayyum, K. Rehman, M. Tariq, M.S.H. Akash, An insight into the emerging role of cyclin-dependent kinase inhibitors as potential therapeutic agents for the treatment of advanced cancers, *Biomedicine & Pharmacotherapy*, 107 (2018) 1326-1341.
- [8] S.R. Walker, M. Xiang, D.A. Frank, Distinct roles of STAT3 and STAT5 in the pathogenesis and targeted therapy of breast cancer, *Molecular and cellular endocrinology*, 382(1) (2014) 616-621.
- [9] S. Eryılmaz, E. Türk Çelikoğlu, Ö. İdil, E. İnkaya, Z. Kozak, E. Mısıır, M. Gül, Derivatives of pyridine and thiazole hybrid: Synthesis, DFT, biological evaluation via antimicrobial and DNA cleavage activity, *Bioorganic chemistry*, 95 (2020) 103476.
- [10] M. ElAwamy, H. Mohammad, A. Hussien, N.S. Abutaleb, M. Hagra, R.A.T. Serya, A.T. Taher, K.A. Abouzid, M.N. Seleem, A.S. Mayhoub, Alkoxyphenylthiazoles with broad-spectrum activity against multidrug-resistant gram-positive bacterial pathogens, *Eur J Med Chem*, 152 (2018) 318-328.
- [11] L. Borkova, I. Frydrych, N. Jakubcova, R. Adamek, B. Liskova, S. Gurska, M. Medvedikova, M. Hajduch, M. Urban, Synthesis and biological evaluation of triterpenoid thiazoles derived from betulonic acid, dihydrobetulonic acid, and ursonic acid, *Eur J Med Chem*, 185 (2020) 111806.

- [12] S. Pathania, R.K. Narang, R.K. Rawal, Role of sulphur-heterocycles in medicinal chemistry: An update, *Eur J Med Chem*, 180 (2019) 486-508.
- [13] S.M. Gomha, K.D. Khalil, A convenient ultrasound-promoted synthesis of some new thiazole derivatives bearing a coumarin nucleus and their cytotoxic activity, *Molecules*, 17(8) (2012) 9335-47.
- [14] S.M. Gomha, N.A. Kheder, M.R. Abdelaziz, Y.N. Mabkhot, A.M. Alhajoj, A facile synthesis and anticancer activity of some novel thiazoles carrying 1,3,4-thiadiazole moiety, *Chemistry Central journal*, 11(1) (2017) 25.
- [15] S.M. Gomha, M.G. Badrey, M.M. Edrees, Heterocyclisation of 2,5-diacetyl-3,4-disubstituted-thieno[2,3-b]Thiophene Bis-Thiosemicarbazones Leading to Bis-Thiazoles and Bis-1,3,4-thiadiazoles as Anti-breast Cancer Agents, *Journal of Chemical Research*, 40(2) (2016) 120-125.
- [16] S.M. Gomha, T.A. Salah, A.O. Abdelhamid, Synthesis, characterization, and pharmacological evaluation of some novel thiadiazoles and thiazoles incorporating pyrazole moiety as anticancer agents, *Monatshefte für Chemie - Chemical Monthly*, 146(1) (2015) 149-158.
- [17] A. Grozav, L.I. Gaina, V. Pileczki, O. Crisan, L. Silaghi-Dumitrescu, B. Therrien, V. Zaharia, I. Berindan-Neagoe, The synthesis and antiproliferative activities of new arylidene-hydrazinyl-thiazole derivatives, *International journal of molecular sciences*, 15(12) (2014) 22059-72.
- [18] T.D. dos Santos Silva, L.M. Bomfim, A.C.B. da Cruz Rodrigues, R.B. Dias, C.B.S. Sales, C.A.G. Rocha, M.B.P. Soares, D.P. Bezerra, M.V. de Oliveira Cardoso, A.C.L. Leite, G.C.G. Militão, Anti-liver cancer activity in vitro and in vivo induced by 2-pyridyl 2,3-thiazole derivatives, *Toxicology and Applied Pharmacology*, 329 (2017) 212-223.
- [19] K. Hu, Z.H. Yang, S.S. Pan, H.J. Xu, J. Ren, Synthesis and antitumor activity of liquiritigenin thiosemicarbazone derivatives, *Eur J Med Chem*, 45(8) (2010) 3453-8.
- [20] W.X. Hu, W. Zhou, C.N. Xia, X. Wen, Synthesis and anticancer activity of thiosemicarbazones, *Bioorganic & medicinal chemistry letters*, 16(8) (2006) 2213-8.
- [21] M. Whittaker, C.D. Floyd, P. Brown, A.J. Gearing, Design and therapeutic application of matrix metalloproteinase inhibitors, *Chemical reviews*, 99(9) (1999) 2735-76.
- [22] S.D. Shapiro, Matrix metalloproteinase degradation of extracellular matrix: biological consequences, *Current opinion in cell biology*, 10(5) (1998) 602-8.
- [23] N.G. Lia, Z.H. Shib, Y.P. Tang, J.A. Duan, Selective matrix metalloproteinase inhibitors for cancer, *Current medicinal chemistry*, 16(29) (2009) 3805-27.
- [24] J.F. Fisher, S. Mobashery, Recent advances in MMP inhibitor design, *Cancer metastasis reviews*, 25(1) (2006) 115-36.
- [25] G. Pochetti, R. Montanari, C. Gege, C. Chevrier, A.G. Taveras, F. Mazza, Extra binding region induced by non-zinc chelating inhibitors into the S1' subsite of matrix metalloproteinase 8 (MMP-8), *J Med Chem*, 52(4) (2009) 1040-9.
- [26] P. Cuniasse, L. Devel, A. Makaritis, F. Beau, D. Georgiadis, M. Matziari, A. Yiotakis, V. Dive, Future challenges facing the development of specific active-site-directed synthetic inhibitors of MMPs, *Biochimie*, 87(3-4) (2005) 393-402.
- [27] T.I. de Santana, M.O. Barbosa, P. Gomes, A.C.N. da Cruz, T.G. da Silva, A.C.L. Leite, Synthesis, anticancer activity and mechanism of action of new thiazole derivatives, *Eur J Med Chem*, 144 (2018) 874-886.
- [28] C.M. Overall, O. Kleifeld, Tumour microenvironment - opinion: validating matrix metalloproteinases as drug targets and anti-targets for cancer therapy, *Nature reviews. Cancer*, 6(3) (2006) 227-39.
- [29] M. Gooyit, W. Song, K.V. Mahasenan, K. Lichtenwalter, M.A. Suckow, V.A. Schroeder, W.R. Wolter, S. Mobashery, M. Chang, O-phenyl carbamate and phenyl urea thiiranes as selective matrix metalloproteinase-2 inhibitors that cross the blood-brain barrier, *J Med Chem*, 56(20) (2013) 8139-50.
- [30] Z.-C. Wang, F.-Q. Shen, M.-R. Yang, L.-X. You, L.-Z. Chen, H.-L. Zhu, Y.-D. Lu, F.-L. Kong, M.-H. Wang, Dihydropyrazothiazole derivatives as potential MMP-2/MMP-8 inhibitors for cancer therapy, *Bioorganic & medicinal chemistry letters*, 28(23) (2018) 3816-3821.

- [31] P.G. Jobin, G.S. Butler, C.M. Overall, New intracellular activities of matrix metalloproteinases shine in the moonlight, *Biochimica et biophysica acta. Molecular cell research*, 1864(11 Pt A) (2017) 2043-2055.
- [32] S.A. Amin, N. Adhikari, T. Jha, Is dual inhibition of metalloenzymes HDAC-8 and MMP-2 a potential pharmacological target to combat hematological malignancies?, *Pharmacological research*, 122 (2017) 8-19.
- [33] A. Jablonska-Trypuc, M. Matejczyk, S. Rosochacki, Matrix metalloproteinases (MMPs), the main extracellular matrix (ECM) enzymes in collagen degradation, as a target for anticancer drugs, *Journal of enzyme inhibition and medicinal chemistry*, 31(sup1) (2016) 177-183.
- [34] N.V. Thomas, P. Manivasagan, S.K. Kim, Potential matrix metalloproteinase inhibitors from edible marine algae: a review, *Environmental toxicology and pharmacology*, 37(3) (2014) 1090-100.
- [35] J.W. Skiles, N.C. Gonnella, A.Y. Jeng, The design, structure, and therapeutic application of matrix metalloproteinase inhibitors, *Current medicinal chemistry*, 8(4) (2001) 425-74.
- [36] J.A. Jacobsen, J.L. Major Jourden, M.T. Miller, S.M. Cohen, To bind zinc or not to bind zinc: an examination of innovative approaches to improved metalloproteinase inhibition, *Biochimica et biophysica acta*, 1803(1) (2010) 72-94.
- [37] M.K. Mazumder, P. Bhattacharya, A. Borah, Inhibition of matrix metalloproteinase-2 and 9 by Piroxicam confer neuroprotection in cerebral ischemia: An in silico evaluation of the hypothesis, *Medical Hypotheses*, 83(6) (2014) 697-701.
- [38] M. Molecular Operating Environment (MOE) Chemical Computing Group, Quebec, Canada. 2012; <http://www.chemcomp.com>. Accessed on 30/02/2013.
- [39] H.E.A. Ahmed, M.F. Zayed, S. Ihmaid, Molecular pharmacophore selectivity studies, virtual screening, and in silico ADMET analysis of GPCR antagonists, *Medicinal Chemistry Research*, 24(9) (2015) 3537-3550.
- [40] A.M. Omar, S. Ihmaid, E.E. Habib, S.S. Althagfan, S. Ahmed, H.S. Abulkhair, H.E.A. Ahmed, The rational design, synthesis, and antimicrobial investigation of 2-Amino-4-Methylthiazole analogues inhibitors of GlcN-6-P synthase, *Bioorganic chemistry*, 99 (2020) 103781.
- [41] B.C. Finzel, E.T. Baldwin, G.L. Bryant, Jr., G.F. Hess, J.W. Wilks, C.M. Trepod, J.E. Mott, V.P. Marshall, G.L. Petzold, R.A. Poorman, T.J. O'Sullivan, H.J. Schostarez, M.A. Mitchell, Structural characterizations of nonpeptidic thiadiazole inhibitors of matrix metalloproteinases reveal the basis for stromelysin selectivity, *Protein Sci*, 7(10) (1998) 2118-2126.
- [42] R. Oltenfreiter, L. Staelens, A. Lejeune, F. Dumont, F. Frankenne, J.-M. Foidart, G. Slegers, New radioiodinated carboxylic and hydroxamic matrix metalloproteinase inhibitor tracers as potential tumor imaging agents, *Nuclear Medicine and Biology*, 31(4) (2004) 459-468.
- [43] G.M. Morris, D.S. Goodsell, R.S. Halliday, R. Huey, W.E. Hart, R.K. Belew, A.J. Olson, Automated docking using a Lamarckian genetic algorithm and an empirical binding free energy function, *Journal of computational chemistry*, 19(14) (1998) 1639-1662.
- [44] H.M. Berman, J. Westbrook, Z. Feng, G. Gilliland, T.N. Bhat, H. Weissig, I.N. Shindyalov, P.E. Bourne, The Protein Data Bank, *Nucleic acids research*, 28(1) (2000) 235-42.
- [45] A. Tochowicz, K. Maskos, R. Huber, R. Oltenfreiter, V. Dive, A. Yiotakis, M. Zanda, T. Pourmotabbed, W. Bode, P. Goettig, Crystal structures of MMP-9 complexes with five inhibitors: contribution of the flexible Arg424 side-chain to selectivity, *Journal of molecular biology*, 371(4) (2007) 989-1006.
- [46] K. Arnold, L. Bordoli, J. Kopp, T. Schwede, The SWISS-MODEL workspace: a web-based environment for protein structure homology modelling, *Bioinformatics (Oxford, England)*, 22(2) (2006) 195-201.
- [47] D.E. Pires, D.B. Ascher, CSM-lig: a web server for assessing and comparing protein-small molecule affinities, *Nucleic acids research*, 44(W1) (2016) W557-61.
- [48] D.E. Pires, T.L. Blundell, D.B. Ascher, pkCSM: Predicting Small-Molecule Pharmacokinetic and Toxicity Properties Using Graph-Based Signatures, *J Med Chem*, 58(9) (2015) 4066-72.

- [49] Y.H. Zhao, J. Le, M.H. Abraham, A. Hersey, P.J. Eddershaw, C.N. Luscombe, D. Boutina, G. Beck, B. Sherborne, I. Cooper, J.A. Platts, Evaluation of human intestinal absorption data and subsequent derivation of a quantitative structure–activity relationship (QSAR) with the Abraham descriptors, *Journal of Pharmaceutical Sciences*, 90(6) (2001) 749-784.
- [50] T. Mosmann, Rapid colorimetric assay for cellular growth and survival: application to proliferation and cytotoxicity assays, *Journal of immunological methods*, 65(1-2) (1983) 55-63.
- [51] F. Demirci, K.H.C. Başer, *Bioassay Techniques for Drug Development By Atta-ur-Rahman, M. Iqbal Choudhary (HEJRIC, University of Karachi, Pakistan), William J. Thomsen (Areana Pharmaceuticals, San Diego, CA). Harwood Academic Publishers, Amsterdam, The Netherlands.* 2001. xii + 223 pp. 15.5 × 23.5 cm. \$79.00. ISBN 90-5823-051-1, *Journal of Natural Products*, 65(7) (2002) 1086-1087.
- [52] A.P. Demchenko, Beyond annexin V: fluorescence response of cellular membranes to apoptosis, *Cytotechnology*, 65(2) (2013) 157-72.
- [53] S.Y. Proskuryakov, V.L. Gabai, Mechanisms of tumor cell necrosis, *Current pharmaceutical design*, 16(1) (2010) 56-68.
- [54] J.M. Coppola, B.D. Ross, A. Rehemtulla, Noninvasive imaging of apoptosis and its application in cancer therapeutics, *Clinical cancer research : an official journal of the American Association for Cancer Research*, 14(8) (2008) 2492-501.
- [55] S.L. Raza, L.A. Cornelius, Matrix metalloproteinases: pro- and anti-angiogenic activities, *The journal of investigative dermatology. Symposium proceedings*, 5(1) (2000) 47-54.
- [56] O. Nyormoi, L. Mills, M. Bar-Eli, An MMP-2/MMP-9 inhibitor, 5a, enhances apoptosis induced by ligands of the TNF receptor superfamily in cancer cells, *Cell death and differentiation*, 10(5) (2003) 558-69.
- [57] P.D. S., K.C. V., V. Kambappa, R.S. R., R. Byregowda, K.Y.C. Sunil, R.S. C., R.K. S., Synthesis and Antileukemic Activity of 1-((S)-2-Amino-4,5,6,7-tetrahydrobenzo[d]thiazol-6-yl)-3-(substituted phenyl)urea Derivatives, 83(6) (2010) 689-697.
- [58] T.I. de Santana, M.d.O. Barbosa, P.A.T.d.M. Gomes, A.C.N. da Cruz, T.G. da Silva, A.C.L. Leite, Synthesis, anticancer activity and mechanism of action of new thiazole derivatives, *European journal of medicinal chemistry*, 144 (2018) 874-886.
- [59] L. Pérez-Martínez, D.M. Jaworski, Tissue Inhibitor of Metalloproteinase-2 Promotes Neuronal Differentiation by Acting as an Anti-Mitogenic Signal, *The Journal of Neuroscience*, 25(20) (2005) 4917.
- [60] M.G. Sans-Fons, S. Sole, C. Sanfeliu, A.M. Planas, Matrix metalloproteinase-9 and cell division in neuroblastoma cells and bone marrow macrophages, *The American journal of pathology*, 177(6) (2010) 2870-85.
- [61] Xu X, Wang Y, Chen Z, Sternlicht MD, Hidalgo M, Steffensen B. Matrix metalloproteinase-2 contributes to cancer cell migration on collagen. *Cancer Res.* 2005; **65**: 130– 6.
- [62] G. Maity, P.R. Choudhury, T. Sen, K.K. Ganguly, H. Sil, A. Chatterjee, Culture of human breast cancer cell line (MDA-MB-231) on fibronectin-coated surface induces pro-matrix metalloproteinase-9 expression and activity, *Tumour biology : the journal of the International Society for Oncodevelopmental Biology and Medicine*, 32(1) (2011) 129-38.
- [63] S. Zheng, Q. Zhong, Y. Xi, M. Mottamal, Q. Zhang, R.L. Schroeder, J. Sridhar, L. He, H. McFerrin, G. Wang, Modification and biological evaluation of thiazole derivatives as novel inhibitors of metastatic cancer cell migration and invasion, *J Med Chem*, 57(15) (2014) 6653-67.
- [64] C.F. Singer, N. Kronsteiner, E. Marton, M. Kubista, K.J. Cullen, K. Hirtenlehner, M. Seifert, E. Kubista, MMP-2 and MMP-9 expression in breast cancer-derived human fibroblasts is differentially regulated by stromal-epithelial interactions, *Breast cancer research and treatment*, 72(1) (2002) 69-77.
- [65] M.W. Roomi, J.C. Monterrey, T. Kalinovsky, M. Rath, A. Niedzwiecki, In vitro modulation of MMP-2 and MMP-9 in human cervical and ovarian cancer cell lines by cytokines, inducers and inhibitors, *Oncology reports*, 23(3) (2010) 605-14.

- [66] M.W. Roomi, J.C. Monterrey, T. Kalinovsky, M. Rath, A. Niedzwiecki, Patterns of MMP-2 and MMP-9 expression in human cancer cell lines, *Oncology reports*, 21(5) (2009) 1323-33.
- [67] P. Vihinen, V.M. Kahari, Matrix metalloproteinases in cancer: prognostic markers and therapeutic targets, *International journal of cancer*, 99(2) (2002) 157-66.
- [68] M. Ii, H. Yamamoto, Y. Adachi, Y. Maruyama, Y. Shinomura, Role of matrix metalloproteinase-7 (matrilysin) in human cancer invasion, apoptosis, growth, and angiogenesis, *Experimental biology and medicine* (Maywood, N.J.), 231(1) (2006) 20-7.
- [69] M. van Engeland, L.J. Nieland, F.C. Ramaekers, B. Schutte, C.P. Reutelingsperger, Annexin V-affinity assay: a review on an apoptosis detection system based on phosphatidylserine exposure, *Cytometry*, 31(1) (1998) 1-9.
- [70] I. Vermes, C. Haanen, H. Steffens-Nakken, C. Reutelingsperger, A novel assay for apoptosis. Flow cytometric detection of phosphatidylserine expression on early apoptotic cells using fluorescein labelled Annexin V, *Journal of immunological methods*, 184(1) (1995) 39-51.
- [71] C. Gercel-Taylor, Diphenylamine assay of DNA fragmentation for chemosensitivity testing, *Methods in molecular medicine*, 111 (2005) 79-82.
- [72] Z. Rihova, L. Sefc, E. Necvas, [Methods used in the detection of apoptosis], *Casopis lekaru ceskych*, 140(6) (2001) 168-72.
- [73] D.M. Boraschi, G., Quantitation of DNA fragmentation with diphenylamine. In *Apoptosis—A Laboratory Manual of Experimental Methods*, Boraschi, D., Bossù, P., Cossarizza, A., Eds.; GCI Publications: L'Aquila, Italy 1998.
- [74] M. Rosner, K. Schipany, M. Hengstschlager, Merging high-quality biochemical fractionation with a refined flow cytometry approach to monitor nucleocytoplasmic protein expression throughout the unperturbed mammalian cell cycle, *Nature protocols*, 8(3) (2013) 602-26.
- [75] A.J. Ridley, Cell migration: Integrating signals from front to back. *Science* 302 (2003) 1704–1709.
- [76] P. Carpintero-Fernandez, New Therapeutic Strategies for Osteoarthritis by Targeting Sialic Acid Receptors. *Biomolecules*. **10**(4) (2020) pii: E637.

Declaration of interests

☒ The authors declare that they have no known competing financial interests or personal relationships that could have appeared to influence the work reported in this paper.

☐The authors declare the following financial interests/personal relationships which may be considered as potential competing interests:

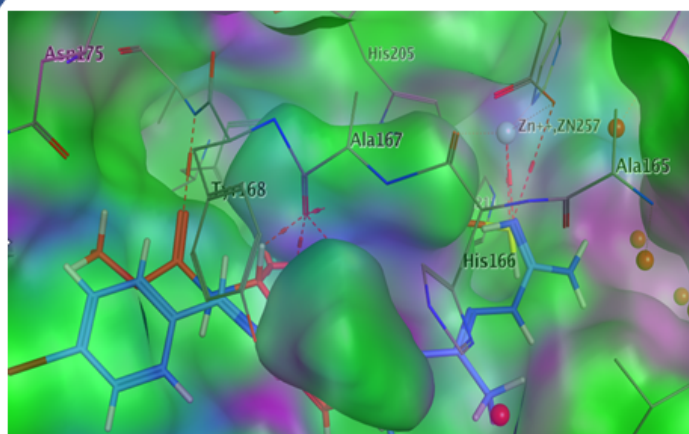
	Journal Pre-proofs

Journal Pre-proofs

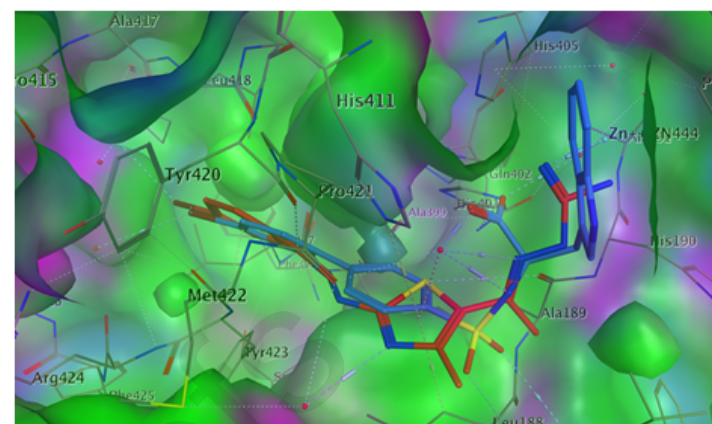
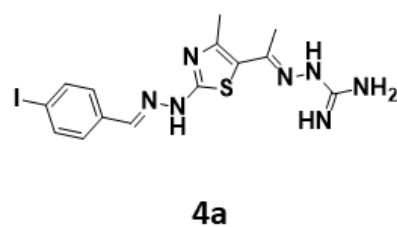
Graphical abstract

Novel Molecular Discovery of Promising Amidine-based thiazole analogues as Potent Dual Matrix Metalloproteinase-2 and 9 Inhibitors: Anticancer Activity Data with Prominent Cell Cycle Arrest and DNA Fragmentation Analysis Effects

Journal Pre-proofs



Matrix Metalloproteinases 2; MMP2
 $IC_{50} = 56 \text{ nM}$



Matrix Metalloproteinases 9; MMP9
 $IC_{50} = 38 \text{ nM}$

Cytotoxicity Profile ($IC_{50} \mu\text{M}$)

MDA-MB-231	HCT-116	MCF-7
0.97 ± 0.03	0.77 ± 0.05	0.02 ± 2.2

Highlights

- 2-Aminothiazoles, linked amidine moieties were synthesized as potential anticancer agents.
- The cytotoxic activity was tested against (MDA-MB-231), (HCT-116) and (MCF-7) cell lines.
- The thiazole-based MMP-2/9 inhibitors have significant potential for anticancer treatment.
- Compounds **4a** were able to induce cell cycle arrest at G2/M phase, cause intrinsic and extrinsic apoptotic cell death.

Journal Pre-proofs

Journal Pre-proofs